AD-A085 825 ANALYTIC SCIENCES CORP READING MA F/G 17/7
SEASONAL SENSITIVITY ANALYSIS OF THE ST. MARY'S RIVER LORAN-C T--ETC(U)
JUN 78 L M DEPALMA, R R GUPTA DOT-CG-81-77-1785
UNCLASSIFIED TASC-TIM 1119-3 USCG-D-33-80 NL

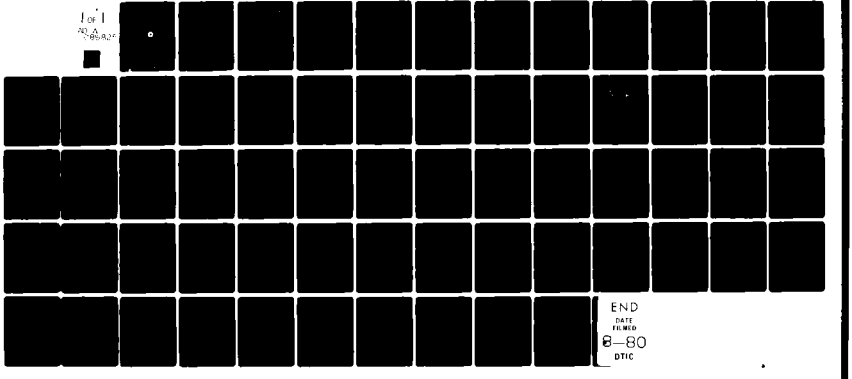

END
DATE FILMED
8-80
DTIC

Report No. CG-D-33-80

LEVEL II

SEASONAL SENSITIVITY ANALYSIS OF THE ST. MARYS RIVER LORAN-C TIME DIFFERENCE GRID

The Analytic Sciences Corporation
6 Jacob Way
Reading, MA 01867

JUNE 1978

INTERIM REPORT

Prepared for

U.S. DEPARTMENT OF TRANSPORTATION
United States Coast Guard
Office of Research and Development
Washington, D.C. 20593

NOTICE

This document is disseminated under the sponsorship of the Department of Transportation in the interest of information exchange. The United States Government assumes no liability for its contents or use thereof.

The contents of this report do not necessarily reflect the official view or policy of the Coast Guard; and they do not constitute a standard, specification, or regulation.

This report, or portions thereof may not be used for advertising or sales promotion purposes. Citation of trade names and manufacturers does not constitute endorsement or approval of such products.

Technical Report Documentation Page

1. Report No.	2. Government Accession No.	3. Recipient's Catalog No.
USCGD-33-80	AD-A085 825	61

4. Title and Subtitle
SEASONAL SENSITIVITY ANALYSIS OF THE ST. MARYS RIVER LORAN-C TIME DIFFERENCE GRID

5. Report Date
Jun[redacted]78

6. Performing Organization Code

7. Author(s)
L.M. DePALMA and R.R. GUPTA

8. Performing Organization Report No.
TASC TIM-1119-3

9. Performing Organization Name and Address
The Analytic Sciences Corporation
6 Jacob Way
Reading, MA 01867

10. Work Unit No. (TRAIS)
2100

11. Contract or Grant No.
DOT-CG-81-77-1785

13. Type of Report and Period Covered
Interim Report,
Mar[redacted] June[redacted]78

12. Sponsoring Agency Name and Address
Department of Transportation
U.S. Coast Guard Research and Development Center
Avery Point
Groton, CT 06340

14. Sponsoring Agency Code
EIB

15. Supplementary Notes

16. Abstract

Large temporal variations have been observed in St. Marys River Loran-C time difference (TD) measurements. As a first step in determing the cause of this instability, the sensitivity of the TD grid to expected seasonal variations in Loran-C signal propagation conditions has been determined. The sensitivity analysis is based on theoretical propagation delay models and expected seasonal variations in the propagation parameters -- surface refractive index of air, the parameter associated with refractive index gradient, and ground conductivity. The analysis results show that conductivity, which is the parameter least amenable to measurement, is also the parameter which is most critical to grid stability. It is shown herein that the assumed variations in conductivity cannot explain observed variations in the TD data. Predicted TD variations due to seasonal grid instability are employed to predict the corresponding position errors at reiver waypoints. The resulting position errors are combined with those predicted for the case of no grid instability (computed in Ref. 1) to provide predictions of total position error.

17. Key Words	18. Distribution Statement
Loran-C, propagation prediction, temporal stability, model calibration, precision navigation, radionavigation	Document is available to the U.S. Public throught the National Technical Information Service, Springfield, VA 22161.

19. Security Classif. (of this report)	20. Security Classif. (of this page)	21. No. of Pages	22. Price
UNCLASSIFIED	UNCLASSIFIED	64	

Form DOT F 1700.7 (8-72) Reproduction of completed page authorized

AD A085565

METRIC CONVERSION FACTORS

Approximate Conversions to Metric Measures

Symbol	When You Know	Multiply by	To Find	Symbol
		LENGTH		
in	inches	*2.5	centimeters	cm
ft	feet	30	centimeters	cm
yd	yards	0.9	meters	m
mi	miles	1.6	kilometers	km
		AREA		
in^2	square inches	6.5	square centimeters	cm^2
ft^2	square feet	0.09	square meters	m^2
yd^2	square yards	0.8	square meters	m^2
mi^2	square miles	2.6	square kilometers	km^2
	acres	0.4	hectares	ha
		MASS (weight)		
oz	ounces	28	grams	g
lb	pounds	0.45	kilograms	kg
	short tons (2000 lb)	0.9	tonnes	t
		VOLUME		
tsp	teaspoons	5	milliliters	ml
Tbsp	tablespoons	15	milliliters	ml
fl oz	fluid ounces	30	milliliters	ml
c	cups	0.24	liters	l
pt	pints	0.47	liters	l
qt	quarts	0.95	liters	l
gal	gallons	3.8	liters	l
ft^3	cubic feet	0.03	cubic meters	m^3
yd^3	cubic yards	0.76	cubic meters	m^3
		TEMPERATURE (exact)		
°F	Fahrenheit temperature	5/9 (after subtracting 32)	Celsius temperature	°C

*1 in = 2.54 (exactly). For other exact conversions and more detailed tables, see NBS Misc. Publ. 286, Units of Weights and Measures. Price $2.25, SD Catalog No. C13.10:286.

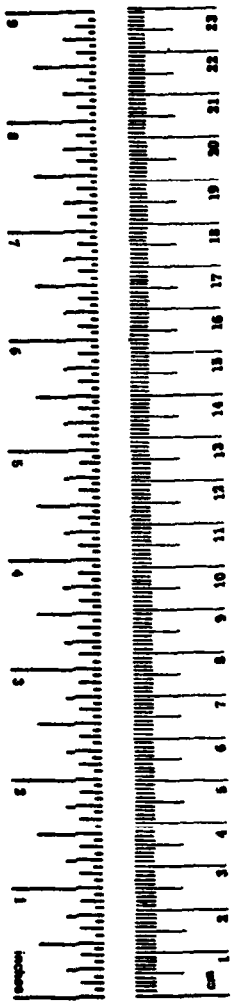

Approximate Conversions from Metric Measures

Symbol	When You Know	Multiply by	To Find	Symbol
		LENGTH		
mm	millimeters	0.04	inches	in
cm	centimeters	0.4	inches	in
m	meters	3.3	feet	ft
m	meters	1.1	yards	yd
km	kilometers	0.6	miles	mi
		AREA		
cm^2	square centimeters	0.16	square inches	in^2
m^2	square meters	1.2	square yards	yd^2
km^2	square kilometers	0.4	square miles	mi^2
ha	hectares (10,000 m^2)	2.5	acres	
		MASS (weight)		
g	grams	0.035	ounces	oz
kg	kilograms	2.2	pounds	lb
t	tonnes (1000 kg)	1.1	short tons	
		VOLUME		
ml	milliliters	0.03	fluid ounces	fl oz
l	liters	2.1	pints	pt
l	liters	1.06	quarts	qt
l	liters	0.26	gallons	gal
m^3	cubic meters	35	cubic feet	ft^3
m^3	cubic meters	1.3	cubic yards	yd^3
		TEMPERATURE (exact)		
°C	Celsius temperature	9/5 (then add 32)	Fahrenheit temperature	°F

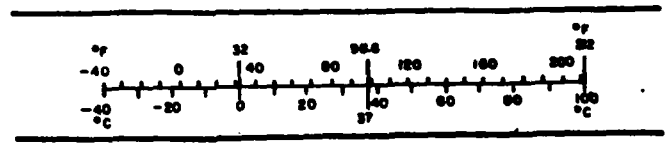

TABLE OF CONTENTS

LIST OF FIGURES

LIST OF TABLES

1. INTRODUCTION

1.1 BACKGROUND AND OBJECTIVES

In the initial phase of this study, a range and bearing (RB)-dependent model was developed to predict the time difference (TD) grid for the St. Marys River Loran-C minichain (Ref. 1). The RB model was calibrated using TD data collected over an 18-day period in September and October 1977*, and therefore exhibits the "average" propagation conditions characterized by the data at that time. Since the chain is expected to provide an all-weather navigation capability, the sensitivity of the TD grid to seasonal variations in propagation conditions is of much interest. In Ref. 1, a comparison of the data collected by the U.S. Coast Guard in November 1977 to that collected in September showed rather large (up to 450 nsec) TD variations at some data collection sites. These observed variations provided additional motivation for the present study, which presents a theoretical sensitivity analysis of the TD grid based on expected seasonal variations in propagation conditions.

1.2 TECHNICAL APPROACH

Figure 1.2-1 presents an overview of the approach employed to predict the variations in the St. Marys River TD grid induced by seasonal changes in propagation conditions. The propagation medium of the Loran-C signal is first characterized by the critical signal propagation parameters. After

*This period is hereafter referred to as September 1977.

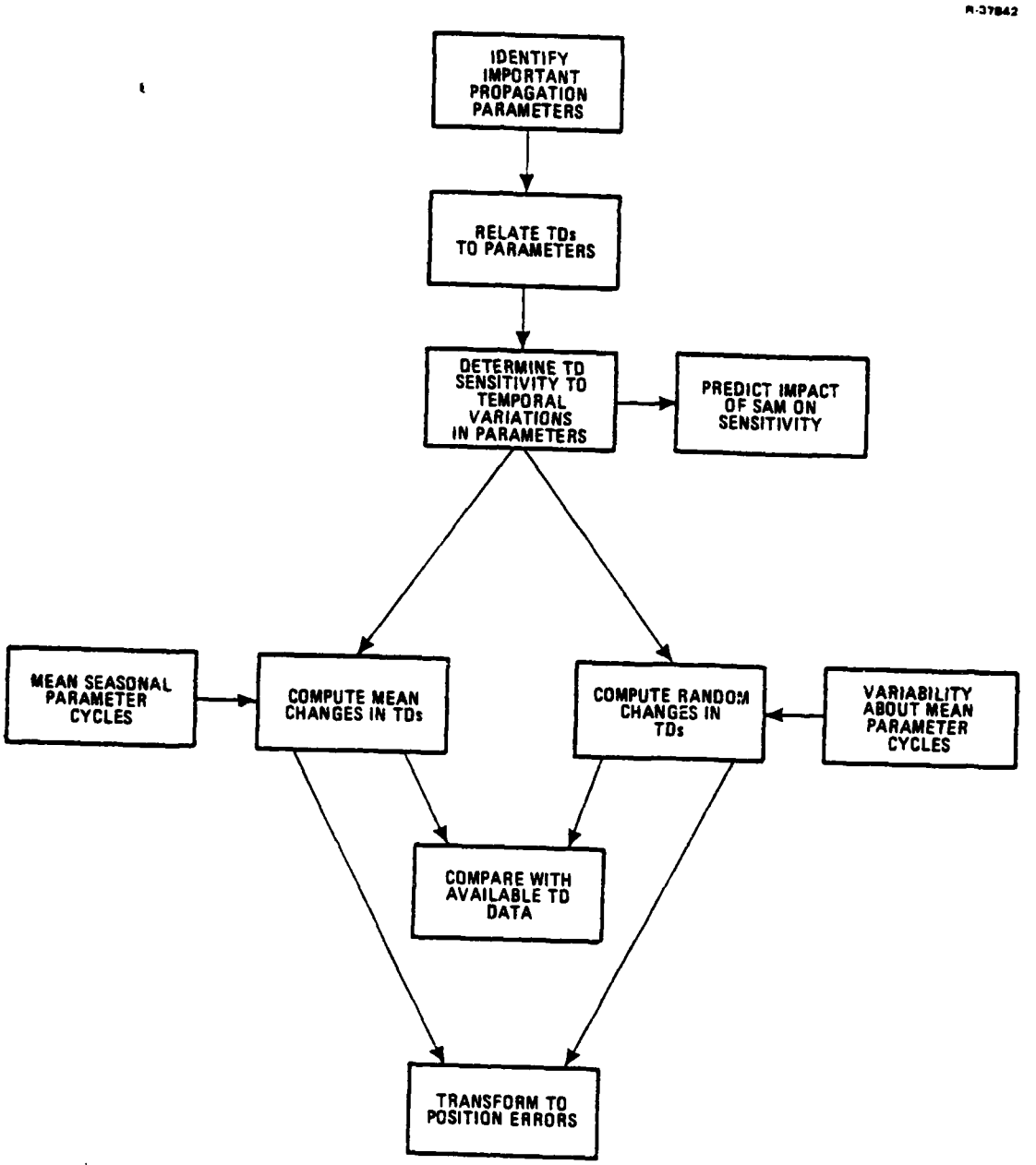

Figure 1.2-1 Sensitivity Analysis Approach

establishing a functional relationship between the parameters and TDs, sensitivity of the grid to changes in propagation parameters is determined. The sensitivity equations reveal the specific role played by the System Area Monitor (SAM) in controlling grid sensitivity (confirming heuristic arguments in Ref. 1).

Next, expected seasonal variations in the propagation parameters are derived from historical meteorological data and other published information. Each parameter is characterized by a mean seasonal cycle and by random fluctuations about this mean cycle encountered over many years. By employing this information in the sensitivity equations, mean and random seasonal TD variations are predicted for the four seasons. A comparison of predicted TD variations with recorded seasonal data shows that propagation theory cannot be used to explain all the observed variations. Preliminary recommendations for a comprehensive data acquisition program are provided, based on the sensitivity analysis.

Position error statistics at St. Marys River waypoints are computed by interpreting seasonal TD variations as uncompensated errors in the calibrated grid. These statistics are compared with similar statistics presented in Ref. 1 to determine the relative contribution of grid instability to position errors.

1.3 REPORT OVERVIEW

The theoretical framework employed to predict TD variations -- including definitions of propagation parameters, the relation between parameters and TDs, and an analysis of the effect of the SAM -- is included in Section 2. In Section 3,

seasonal variations in propagation parameters are inferred from available information, and TD and position errors resulting from the variations are determined. Conclusions and recommendations of the study are summarized in Section 4. Detailed equations and tables are presented in the appendices.

2. PROPAGATION MODELS AND SENSITIVITY ANALYSIS

2.1 INTRODUCTION

The range and bearing-dependent model calibrated in Ref. 1 is a semi-empirical characterization of the St. Marys River Loran-C time difference grid. Although the functional structure of the model is based on classical propagation theory (Ref. 2), it does not explicitly include the propagation parameters. The model coefficients were chosen to minimize the residuals between predicted and measured TDs, thereby characterizing the grid which existed during the September 1977 data collection period. Since the model does not explicitly include all important propagation parameters, it cannot be used directly in a seasonal sensitivity analysis.

Two alternate approaches to seasonal sensitivity analysis have been considered:

- Calibrate a time-dependent TD prediction model which includes the important propagation parameters, using seasonal TD data
- Utilize a model of a homogeneous smooth earth to estimate gross changes in the TD grid due to uniform changes in propagation parameters.

The former approach would be capable of accounting for spatial detail of the ground conductivity, through a bearing dependence as in the RB model or through some similar artifice. However, this requires a more extensive data base than is presently available. The latter approach, although not addressing changes

in spatial detail explicitly, has been chosen here for its tractability. The model is not calibrated against seasonal data but rather stands on theory alone.

2.2 ACCURACY OF CALIBRATED TD GRID

The role of the RB model in predicting the St. Marys River Loran-C TD grid is reviewed in this section. The true time difference (TD_i), between signals from secondary station i and the master station m, is assumed to be measured by a perfect receiver in a noiseless environment (this ideal condition is referred to as zero measurement noise). If propagation delays between the stations and the user are denoted by PD_i and PD_m and the secondary station emission delay by ED_i, then

$$TD_i = PD_i - PD_m + ED_i \qquad (2.2\text{-}1)$$

All variables in Eq. 2.2-1 may vary temporally at a fixed user location.

In Ref. 1, the true time difference is conceptually separated into three components:

- A portion which can be described by the RB model structure, termed the spatial-area TD, $\overline{TD}_i$
- A portion due to unmodelled spatial details which do not change with time, termed the local warpage, δTD_i
- A portion due to temporal variations in propagation conditions, termed the temporal grid instability, ΔTD_i.

The RB model predicts the spatial-area TDs which existed during September 1977 data collection (RB model-predicted TD, denoted by $\hat{TD}_i$). The error incurred in estimating the spatial-area TD

(termed residual grid prediction error or $\delta\overline{TD}_i$) depends on the quality and quantity of data used to calibrate the RB model. This error was predicted at the waypoints by covariance analysis in Ref. 1. The total TD prediction error (difference between the predicted and measured TD, in the absence of measurement noise) when the RB model is employed to predict the true time difference is then

$$\text{Total TD error} = TD_i - \hat{TD}_i = \delta\overline{TD}_i + \delta TD_i + \Delta TD_i \qquad (2.2\text{-}2)$$

The primary purpose of this study is to predict seasonal statistics for temporal grid instability. However, during the course of computing total position errors, local warpage errors are hypothesized based on available information.

2.3 PROPAGATION PARAMETERS AND THEORETICAL PHASE DELAY MODEL

Signal propagation theory (Ref. 2) and published observations (Refs. 4 and 5) show that the characteristics of Loran-C groundwave propagation can be described by the following propagation parameters:

- Surface atmospheric refractive index, n
- A parameter α, which is related to the refractive index gradient
- Ground conductivity, σ_c.

The parameters vary both spatially and temporally in the St. Marys River Loran-C coverage area. However, the classical propagation model used herein assumes a homogeneous smooth earth, an idealization of the true propagation medium.

Classical theory for a homogeneous medium expresses the groundwave signal phase delay* as the sum of a primary phase delay (T) and a secondary phase delay, also known as secondary phase factor, SF†. The primary phase delay is experienced in an atmosphere with refractive index n, in the absence of the earth, while the secondary phase delay describes the additional effect of the earth. The theoretical time difference is therefore given by

$$TD_i = (T_i - T_m) + (SF_i - SF_m) + ED_i \qquad (2.3\text{-}1)$$

In Sections 2.3.1 to 2.3.3, the relationships between the propagation parameters and the components of phase delay are presented. Then, in Section 2.4, TD sensitivity to changes in the parameters is derived from Eq. 2.3-1.

2.3.1 Surface Refractive Index

The wave velocity in an atmosphere of refractive index n (dimensionless) is reduced from the velocity in free space (c in ft/μsec) by the factor 1/n. Hence, the primary phase delay (μsec) along a geodesic of length R (ft) is

$$T = \left(\frac{n}{c}\right) R \qquad (2.3\text{-}2)$$

Secondary phase delay is approximately proportional to $n^{1/3}$ (Ref. 2). Therefore, changes in SF are given by

$$\Delta SF = \frac{SF}{3}\left(\frac{\Delta n}{n}\right) \qquad (2.3\text{-}3)$$

*Phase delay ϕ is normally expressed in units of time through the conversion $\phi/2\pi f$, where f is the 100 Khz Loran-C carrier frequency.
†Herein SF denotes the total secondary phase factor for any land/water path and not the SF associated with an equivalent sea water path.

Since changes in primary phase delay (from Eq. 2.3-2) are given by

$$\Delta T = T \frac{\Delta n}{n} \qquad (2.3\text{-}4)$$

and T>>SF/3 for ranges of interest in the St. Marys River coverage area, the effect of changes in the refractive index on SF can be ignored.

2.3.2 Parameter α

The parameter α (dimensionless) is an artifice used in signal propagation theory to account for wave refraction due to the refractive index gradient, dn/dh (where h is altitude). For an earth of radius a, the parameter is computed by evaluating

$$\alpha = 1 + \frac{a}{n} \frac{dn}{dh} \qquad (2.3\text{-}5)$$

at the earth's surface (h=0). The parameter α affects secondary phase delay in a complex manner (see Ref. 2 for details). However, over ranges of interest in the St. Marys River Loran-C coverage area (<100 mi), the following relation provides a reasonable approximation to the classical model:

$$SF(\alpha) = SF(\alpha_o) + 0.0005\ (\alpha-\alpha_o)\ T \qquad (\mu sec) \qquad (2.3\text{-}6)$$

where α_o is a nominal value of α (chosen equal to 0.75, to lie in the expected range for the St. Marys River region) and T is defined by Eq. 2.3-2.

2.3.3 Ground Conductivity

Ground conductivity σ_c (mho/m) is the most important parameter in the theoretical formulation of secondary phase delay, encompassing all non-atmospheric effects. The theore-

tical relationship between secondary phase delay and conductivity, detailed in Ref. 2, is too cumbersome to apply in sensitivity analyses. Therefore, an alternative relationship has been derived which is only applicable to the signal path lengths (1-100 mi) and conductivities (0.001-0.01 mho/m, see Section 3.2.3) relevant to the St. Marys River region. The following polynomial was fit to "samples" of secondary phase delay computed from classical theory:

$$SF = \sum_{k=-2}^{2} \sum_{\ell=-1}^{1} A_{k\ell} \, \xi^{\ell} \, T^{k} \qquad (2.3\text{-}7)$$

where

SF = secondary phase delay (μsec)
T = primary phase delay (μsec)
ξ = natural logarithm of conductivity, σ_c (mho/m)
$A_{k\ell}$ = least-squares-derived coefficients listed in Table 2.3-1.

TABLE 2.3-1
COEFFICIENTS $A_{k\ell}$ OF POLYNOMIAL SF MODEL

k \ ℓ	-1	0	1
-2	-106.2	-58.80	-9.115
-1	33.12	21.18	2.850
0	-3.766	-2.139	-0.3279
1	-0.02380	-0.01380	-0.002257
2	1.565×10^{-5}	9.369×10^{-6}	1.456×10^{-6}

Since the coefficients $A_{k\ell}$ were computed based on the nominal value of α ($\alpha_o = 0.75$), the secondary phase delay defined by Eq. 2.3-7 is the nominal delay, $SF(\alpha_o)$, appearing in Eq. 2.3-6. Figure 2.3-1 illustrates the relationship between SF and T, computed from Eq. 2.3-7, for two pertinent values of conductivity. Polynomials similar to Eq. 2.3-7 have been employed in other Loran-C studies, such as described in Ref. 6.

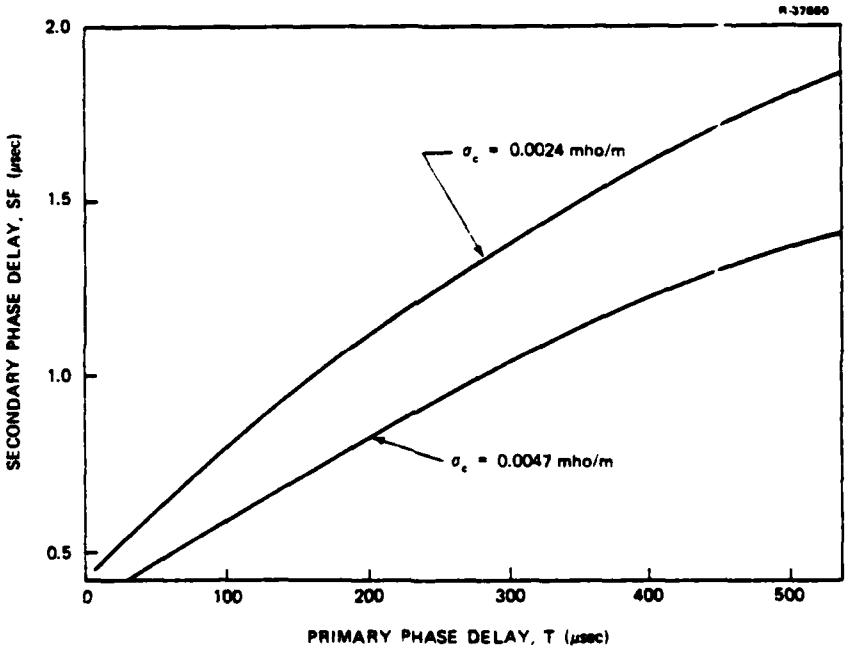

Figure 2.3-1 Secondary Phase Delay as a Function of Primary Phase Delay for Two Conductivities

2.4 SENSITIVITY EQUATIONS AND THE EFFECT OF SAM

In Section 2.3, the relationship between TDs and the propagation parameters of a homogeneous medium was established. Before Eq. 2.3-1 can be applied to determine the sensitivity of TDs to temporal variations in the propagation parameters, the secondary station emission delay (see Eq. 2.2-1) must be related to the parameters.

Emission delay, ED_i, is the time between transmission of the master pulse group and the secondary pulse group. The System Area Monitor (SAM) controls emission delay through coding delay adjustments transmitted to the secondary station. These adjustments are chosen so that the TD measured at SAM equals a prescribed reference (TD_i^o) with a tolerance of ±15 nsec. If SAM were capable of controlling its received TDs precisely, then from Eq. 2.3-1

$$ED_i = TD_i^o - (T_i'-T_m') - (SF_i'-SF_m') \qquad (2.4\text{-}1)$$

where prime (') distinguishes SAM phase delays from user phase delays. Note that the emission delay varies if the propagation parameters of the medium vary. By combining Eqs. 2.3-1 and 2.4-1, the effect of propagation parameters and SAM on the TDs at a user location is shown to be

$$TD_i = \left[(T_i-T_m) + (SF_i-SF_m)\right] - \left[(T_i'-T_m') + (SF_i'-SF_m')\right] + TD_i^o \qquad (2.4\text{-}2)$$

Note that a user positioned at SAM measures TD_i^o.

Equation 2.4-2 can be employed directly in sensitivity analyses to predict ΔTD_i, the temporal grid instability (see Section 2.2) arising from a particular temporal change in propagation parameters. If subscripts 1 and 2 denote two different parameter sets, then

$$\Delta TD_i = TD_i(n_2,\alpha_2,\xi_2) - TD_i(n_1,\alpha_1,\xi_1) \qquad (2.4\text{-}3)$$

If random changes are of interest, it is more convenient to use the following linear approximation in a covariance analysis:

$$\Delta TD_i = \frac{\partial TD_i}{\partial n}\Delta n + \frac{\partial TD_i}{\partial \alpha}\Delta\alpha + \frac{\partial TD_i}{\partial \xi}\Delta\xi \qquad (2.4\text{-}4)$$

The required partial derivatives of TD with respect to the parameters follow from Eq. 2.4-2, using the relations

$$\frac{\partial T}{\partial n} = T/n$$

$$\frac{\partial SF}{\partial \alpha} = 0.0005\ T$$

$$\frac{\partial SF}{\partial \xi} = \sum_{k=-2}^{2} \sum_{\ell=-1}^{1} A_{k\ell}\ \ell\ \xi^{\ell-1}\ T^{k} \qquad (2.4\text{-}5)$$

Figure 2.4-1 shows the variation of the derivative of SF with respect to ξ with T, for two values of conductivity referred to later herein. The convenient approximation

$$\frac{\partial SF}{\partial \xi} = -0.039\ T^{0.47} \qquad (2.4\text{-}6)$$

differs from the plotted values by less than five percent for both values of conductivity.

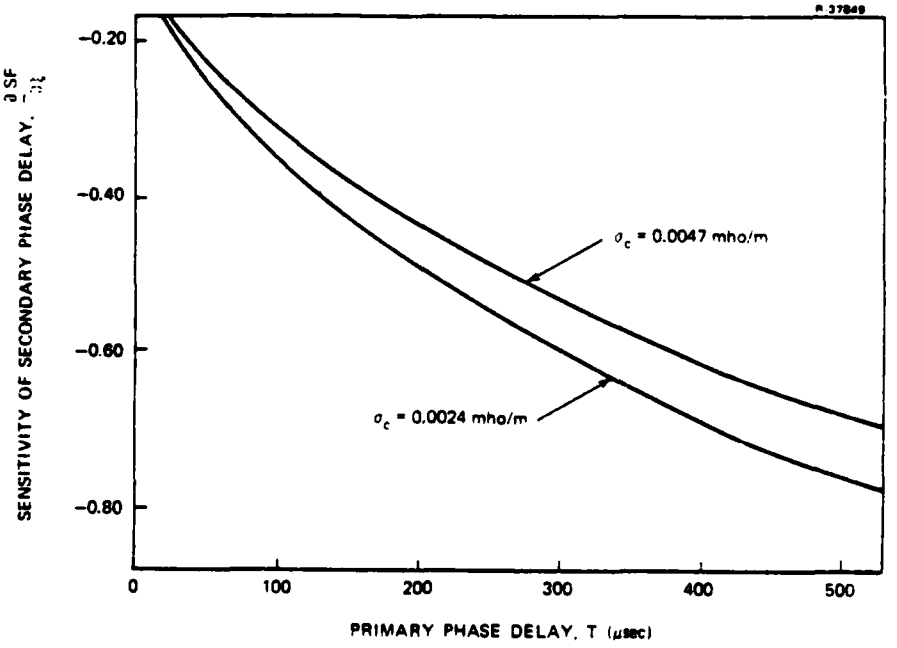

Figure 2.4-1 Sensitivity of Secondary Phase Delay to ℓn (Conductivity)

Equations 2.4-2 to 2.4-6 can be used to relate parameter variations to expected TD changes and are referred to as the sensitivity equations. The following observations can be made from the sensitivity equations:

- The reference TD prescribed for SAM does not affect sensitivity
- The SAM removes all sensitivity of TDs to the relative drift of the master and secondary clocks
- SAM decreases the sensitivity of TDs to propagation parameter variations at some user locations, while increasing sensitivity at others.*

The impact of SAM on TD sensitivity to variations in refractive index and the parameter α is determined by the primary phase delay differences at the user $(T_i - T_m)$ and at the SAM $(T_i' - T_m')$. SAM increases the magnitude of the TD sensitivity to n and α at those user locations where

- The primary phase differences at the user and SAM are of opposite sign
- The primary phase differences are the same sign but $|T_i - T_m| < 0.5|T_i' - T_m'|$.

SAM decreases the TD sensitivity at all other locations in the coverage area, reducing the sensitivity to zero along the SAM LOP. In other words, because SAM is controlling the chain to hold the LOPs through SAM constant, TD variations due to propagation parameter changes are removed by SAM and a user on the SAM LOP will not observe the effects of these parameter variations (within the $\pm$15 nsec control tolerance). Consequently, the associated TD sensitivity to parameter changes is zero. However, there is a locus of points in the coverage region, for each TD, along which the magnitude of the TD

*This conclusion was arrived at in Ref. 1 by assuming a linear dependence of phase delay on a propagation parameter.

sensitivity is the same with SAM as without SAM. This is not to say that the TD sensitivity is zero and that a user will not observe TD variations along the locus of points. In fact, the sense of the TD sensitivity changes if SAM is active or inactive but the absolute value of the sensitivity remains constant. In Fig. 2.4-2, the St. Marys River region is divided into regions (for each TD) where SAM increases or decreases the TD sensitivity to variations in n and α. From these charts it is evident that SAM increases grid sensitivity to variations in n and α at many waypoints in the southern region of the river.

The sensitivity of TDs to temporal variations in the conductivity of a homogeneous medium is nonlinear in T, as shown by Eq. 2.4-6. Therefore, the boundary lines in Fig. 2.4-2 are not precisely applicable to conductivity. In Fig. 2.4-3, the sensitivity of TDs to conductivity variations is plotted versus waypoint, for cases with SAM and without SAM. The following observations are derived from these sensitivity curves:

- TDX* is the least sensitive TD. Although SAM increases the sensitivity to conductivity variations at most waypoints, sensitivity is decreased to near zero between waypoints I and M, a region where the channel narrows to 300 ft
- SAM greatly reduces the sensitivity of TDY to variations in conductivity north of waypoint W. However, south of waypoint W, sensitivity is greatly increased. Note that MXY is the preferred station triad south of waypoint W because of low geometric dilution of precision
- SAM has little impact on the sensitivity of TDZ to variations in conductivity.

*TDX, TDY and TDZ are the respective TDs associated with the x, y and z secondary stations.

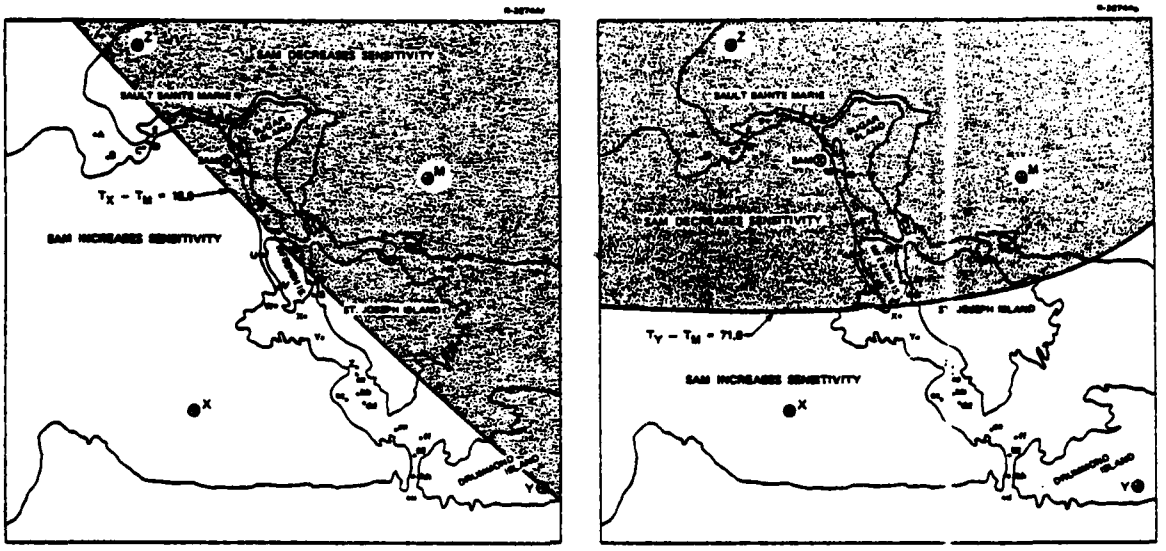

a) TDX

b) TDY

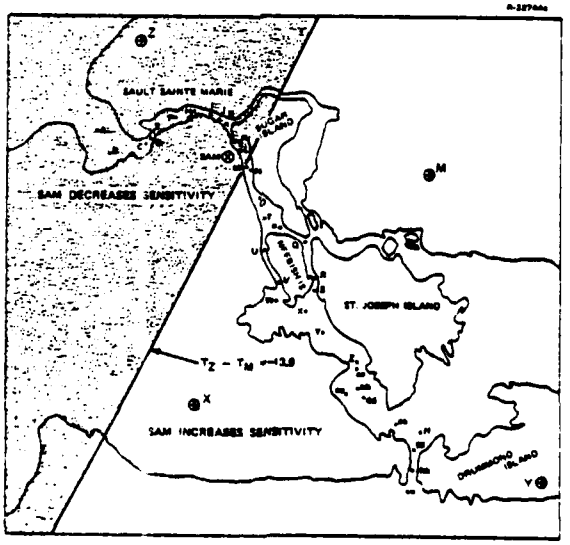

c) TDZ

Figure 2.4-2 Regions Where SAM Increases and Decreases Sensitivity of TDs to Variations in n and α

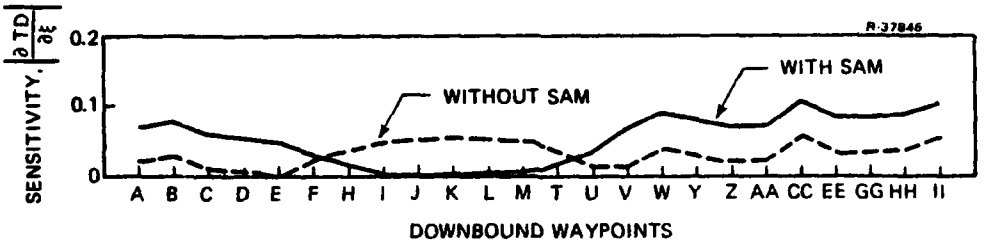

(a) TDX

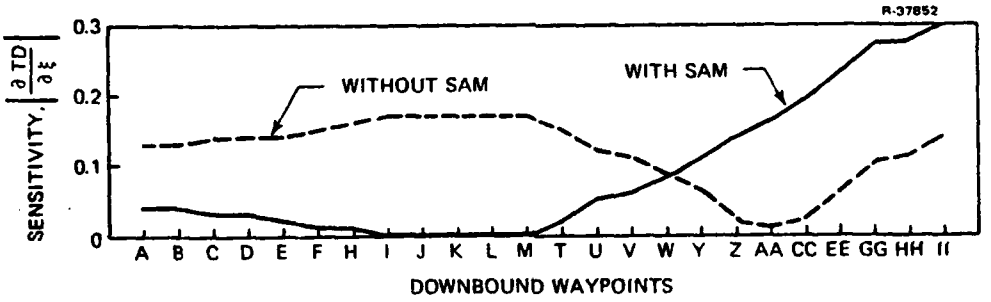

(b) TDY

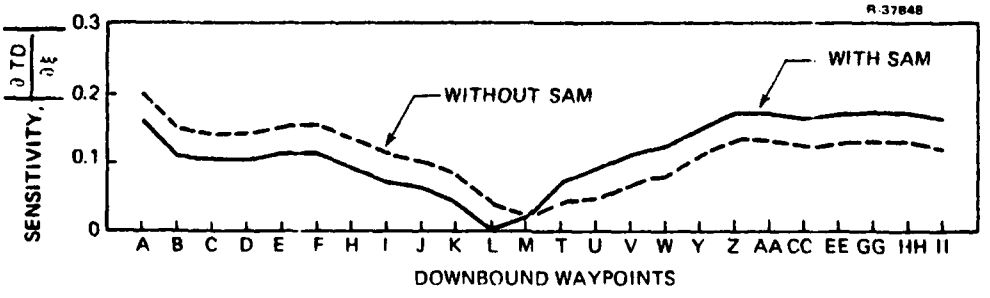

(c) TDZ

Figure 2.4-3 TD Sensitivity to ℓn (Conductivity) With SAM and Without SAM

When these results are compared to Fig. 2.4-2, it is found that Fig. 2.4-2 correctly displays the effect of SAM on TD sensitivity to conductivity at the waypoints. Figure 2.4-2 may therefore be used with confidence, in the vicinity of the river, for refractive index, the parameter α and conductivity.

Although the analysis herein suggests that the SAM can promote temporal grid instability at some locations due to variations in propagation parameters, the SAM is nevertheless critical to controlling relative errors between secondary and master station clocks. A possible remedy of this situation may be to establish other SAMs in the service area and to utilize information from all SAMs to derive local phase adjustments. By employing optimal estimation theory, it may be possible to reduce grid sensitivity to parameter variations beyond what is possible with a single SAM. The predictions of seasonal grid variations presented in Section 3 utilize the present SAM location and operating procedure.

3. PREDICTED SEASONAL VARIATIONS IN THE ST. MARYS RIVER LORAN-C GRID

3.1 INTRODUCTION

In Section 2, TD sensitivity equations for the propagation parameters n, α, and σ_c are derived from theoretical considerations. These equations permit the prediction of TD variations corresponding to expected propagation parameter variations. In this section, historical meteorological data and other published information are used to describe the variation of each parameter by a mean seasonal cycle and random deviations from this cycle. Expected mean and random TD variations are then computed, using the sensitivity equations, and compared with temporal TD variations observed in the St. Marys River chain data collected by the U.S. Coast Guard. The impact of predicted seasonal TD variations on a Loran-C user employing the calibrated TD grid is given in terms of expected position errors at river waypoints.

3.2 EXPECTED VARIATIONS IN PROPAGATION PARAMETERS

The propagation parameters n, α, and σ_c vary in space and time in the St. Marys River Loran-C service area. In order to satisfy the requirement of a homogeneous medium (adopted in Section 2 for tractability), spatial averages for the parameters must be determined. Sections 3.2.1 to 3.2.3 present seasonal variations of the spatial averages.

3.2.1 Surface Refractive Index

The refractive index n, which impacts primary phase delay as discussed in Section 2.3.1, can be determined from surface meteorological parameters. Since the refractive index of air does not exceed unity by more than a few parts in 10^4, it is convenient to consider instead the refractivity

$$N = (n-1) \times 10^6 \qquad (3.2\text{-}1)$$

which is of the order of 300 units. Refractivity is related to atmospheric pressure p (mbar), absolute temperature T (^{o} Kelvin), and relative humidity RH (%) by the formula (Ref. 7):

$$N = 77.6 \left(\frac{p}{T}\right) + 3730.0 \left(\frac{e_s \, RH}{T^2}\right) \qquad (3.2\text{-}2)$$

where e_s denotes saturation water vapor pressure at temperature T. The first and second terms of Eq. 3.2-2 correspond to the "dry" and "wet" components of N, respectively.

Data from the National Weather Service Station at Sault Sainte Marie, Michigan are assumed to be representative of weather conditions in the St. Marys River region for purposes of determining seasonal variations of refractivity. Equation 3.2-2 has been employed in Ref. 8 to compute monthly statistics for N at Sault Sainte Marie (by hour) from meteorological data collected over an eight-year period. In Fig. 3.2-1, the mean seasonal cycle and $\pm 1\sigma$ bounds along with the extreme bounds are plotted for 12 o'clock noon local standard time. These data reveal a distinct seasonal cycle with a relatively narrow 1σ spread. Furthermore, refractivity statistics versus time of day for each month (August, for example, is given in Fig. 3.2-2) show that seasonal variations are only slightly dependent on the time of day.

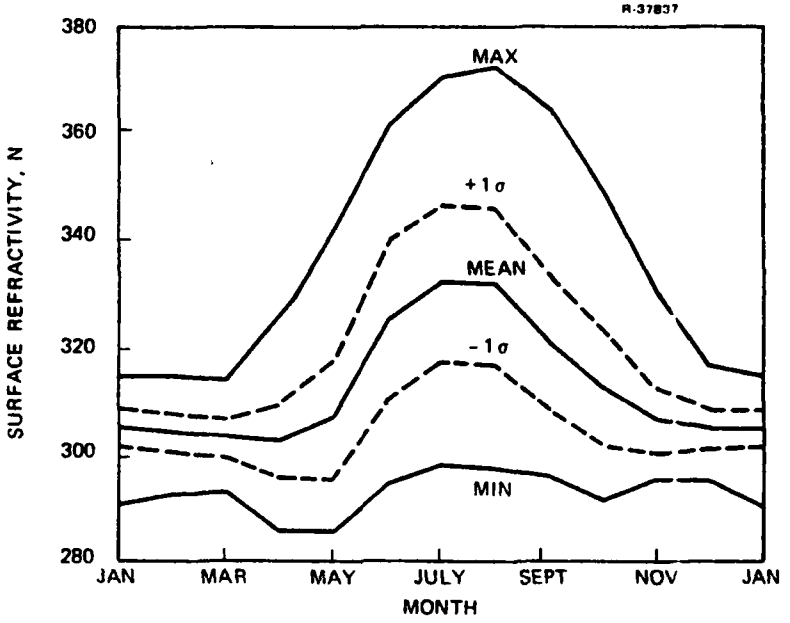

Figure 3.2-1 Historical Seasonal Variations of Refractivity at Sault Sainte Marie Weather Station

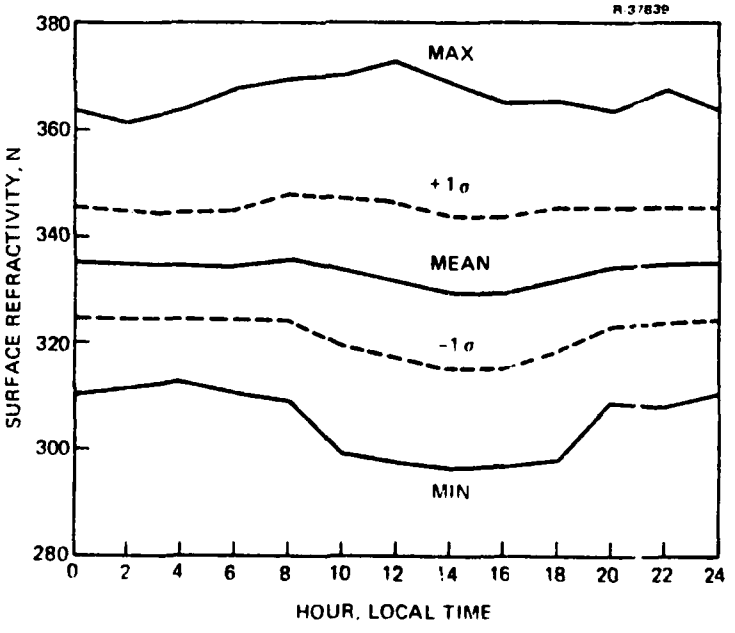

Figure 3.2-2 Historical Diurnal Variations of Refractivity at Sault Sainte Marie During August

The average refractivity for the 18-day September 1977 data collection period is 324.0 at Sault Sainte Marie, compared to the computed mean of 331.0 at the data collection sites. Sault Sainte Marie data is employed consistently herein because continuous weather data are not available at the sites. Note that although neither Sault Sainte Marie nor the sites necessarily exhibit the average refractivity of the coverage area, the refractivity is within the 1σ bounds associated with the month of September shown in Fig. 3.2-1.

3.2.2 Parameter α

The propagation parameter α, which affects secondary phase delay as discussed in Section 2.3.2, depends on the vertical lapse rate of the refractive index, i.e., dn/dh. The lapse rate is commonly interpreted as the change in n between the surface and a 1 km altitude. If the corresponding change in refractivity is ΔN, then Eq. 2.3-5 becomes

$$\alpha = 1 + 0.006363 \left(\frac{\Delta N}{n}\right) \qquad (3.2\text{-}3)$$

For most meteorological conditions (excluding temperature inversions), ΔN is negative and highly correlated with surface refractivity. In Ref. 9, the following regression equation was fit to 888 pairs of data from 45 U.S. weather stations

$$\Delta N = -7.32\, e^{0.005577\, N} \qquad (3.2\text{-}4)$$

The resulting high correlation coefficient (0.93) justifies computing ΔN from surface meteorological data alone, in the absence of radiosonde data from 1 km altitude.

Although radiosonde data at Sault Sainte Marie are employed in Ref. 7 to determine a mean seasonal cycle for

ΔN, the data records necessary to determine 1σ and extreme bounds are not readily obtainable. Therefore, Eq. 3.2-4 is employed to transform the statistics of surface refractivity to statistics for ΔN, resulting in the seasonal variations plotted in Fig. 3.2-3. The mean seasonal cycle computed in this manner agrees closely with the radiosonde data of Ref. 7. The average value of ΔN at Sault Sainte Marie for the September 1977 data collection period is -45.

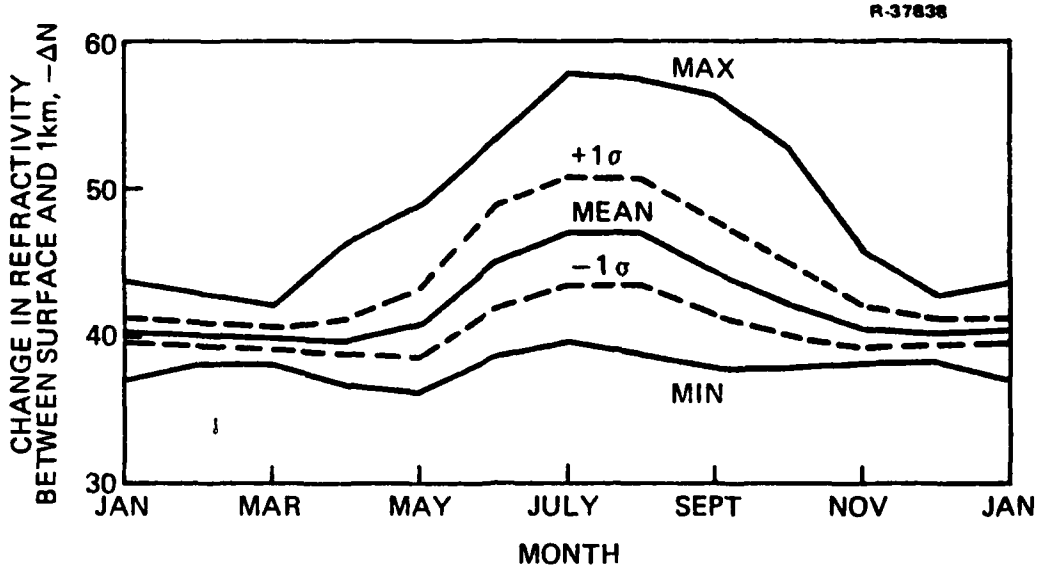

Figure 3.2-3 Seasonal Variations of ΔN at Sault Sainte Marie

3.2.3 Ground Conductivity

Unlike the atmospheric parameters n and α, ground conductivity σ_c (mho/m) cannot be easily related to physical parameters and must be inferred from signal propagation data. Although no known published conductivity data is available near Loran-C frequencies (90-110 KHz) for the St. Marys River region, data at other frequencies are reported in Refs. 10-13.

Since conductivity varies little with frequency below 10 MHz (Ref. 10), published data are employed to establish an expected conductivity range of 0.001 mho/m to 0.01 mho/m for the St. Marys River Loran-C application. The "average" ground conductivity of interest here is that associated with station-to-user signal propagation paths. Since determination of the average conductivity for the region from the limited information cited above is impractical and unwarranted, the conductivity has been estimated from the September 1977 Loran-C data.

The parameters n and α are assumed constant at their known average values for the period, and σ_c is estimated using the homogeneous Loran-C signal propagation model established in Section 2.3. A value of 0.0047 mho/m for the parameter σ_c has been identified from the September 1977 U.S. Coast Guard TD data by maximum likelihood estimation techniques (Ref. 14) which are conveniently embodied in TASC software PARAIDE. The resulting homogeneous model is not a replacement for the RB model, as it yields much larger residual TDs. However, the calibrated conductivity (0.0047 mho/m) serves as a baseline, to be used with other published information to provide expected seasonal conductivity variations. It must be remembered that 0.0047 mho/m has been derived from data and, therefore, is "tuned" to the specific propagation conditions inherent in the data. In addition, the estimate may be influenced by measurement noise.

Since the spatial-average conductivity for the region is not expected to vary appreciably except in winter, the mean of the spatial-average conductivities over many years is assumed equal to 0.0047 mho/m for spring, summer and fall. The random variability in the conductivity from year to year for these three seasons is estimated by assuming that the published range of conductivities over space (0.001 to 0.01 mho/m) is the same range encountered in the spatial-average

conductivity from year to year. If this range defines a 3σ spread for spring, summer and fall conductivities, then the 1σ factor* for conductivity is 1.5 and the 1σ spread is 0.0031 to 0.0071 mho/m.

A significant decrease in conductivity is expected during winter in the St. Marys River region due to snow and ice ($\approx 3.0 \times 10^{-5}$ mho/m) and frozen ground ($\approx 10^{-4}$ mho/m), which have lower conductivities (Ref. 15) than average ground (≈ 0.001 mho/m). A two-layer earth model (Ref. 16) has been employed to estimate the effective conductivity for 1-2 m of snow or frozen ground on top of average ground, and 1 m of ice on fresh water. The minimum calculated conductivity was 0.00057 mho/m, for snow on average ground. Thus, the range of conductivities over the region for all winters, including mild winters, is expected to be 0.00057 to 0.01 mho/m. The geometrical mean of the extremes, 0.0024 mho/m, is employed as the mean spatial-average conductivity for winter. Since the extent of ice, snow and frozen ground can vary greatly from winter to winter, the expected range is interpreted only as a 2σ spread. The resulting 1σ conductivity factor is 2 and the 1σ spread is 0.0012 to 0.0048 mho/m. The seasonal variations in the TD grid presented in the next section should be recomputed if better estimates of conductivity variations can be determined.

3.3 EXPECTED VARIATIONS IN TDs

In Table 3.3-1, statistics of seasonal parameter variations estimated in Section 3.2 are summarized for four times of the year, corresponding approximately to the middle of the four seasons. The mean cycle is an *a priori* estimate of seasonal parameter changes while the standard deviation (1σ)

*A 1σ factor of 1.5 implies that the standard deviation of $\ell n\ \sigma_c$ is $\ell n\ 1.5$. The 1σ spread about the mean $\overline{\sigma}_c$ is $\overline{\sigma}_c / 1.5$ to $1.5\ \overline{\sigma}_c$.

TABLE 3.3-1
EXPECTED SEASONAL VARIATION OF PARAMETERS

Season	n		α		σ_c (mho/m)	
	Mean	1σ(x10^6)	Mean	1σ	Mean	1σ Factor
Spring	1.000305	11	0.76	0.02	0.0047	1.5
Summer	1.000328	16	0.70	0.03	0.0047	1.5
Fall	1.000312	13	0.73	0.03	0.0047	1.5
Winter	1.000304	4	0.77	0.01	0.0024	2.0
September 1977	1.000324	-	0.70	-	0.0047	-

indicates the random fluctuation about the mean cycle over many years. Also indicated in Table 3.3-1 are the parameter values for the period during September 1977 when the TD data used to calibrate the RB model were collected. The primary objective is to present statistics for TD variations at the river waypoints corresponding to expected variations in the propagation parameters n, α, and σ_c. The sensitivity equations, which relate TD variations to parameter variations, were derived in Section 2 and are summarized in Appendix A.

3.3.1 Mean Seasonal TD Shifts

The mean TD shift for each season is the expected change in TD experienced if all three propagation parameters change from their values during the September 1977 data collection period to the assumed mean values for the season. Mean winter TD shifts are illustrated for downbound river waypoints in Fig. 3.3-1, and mean TD shifts for all seasons and all waypoints are tabulated in Appendix C (Tables C-1 to C-4).

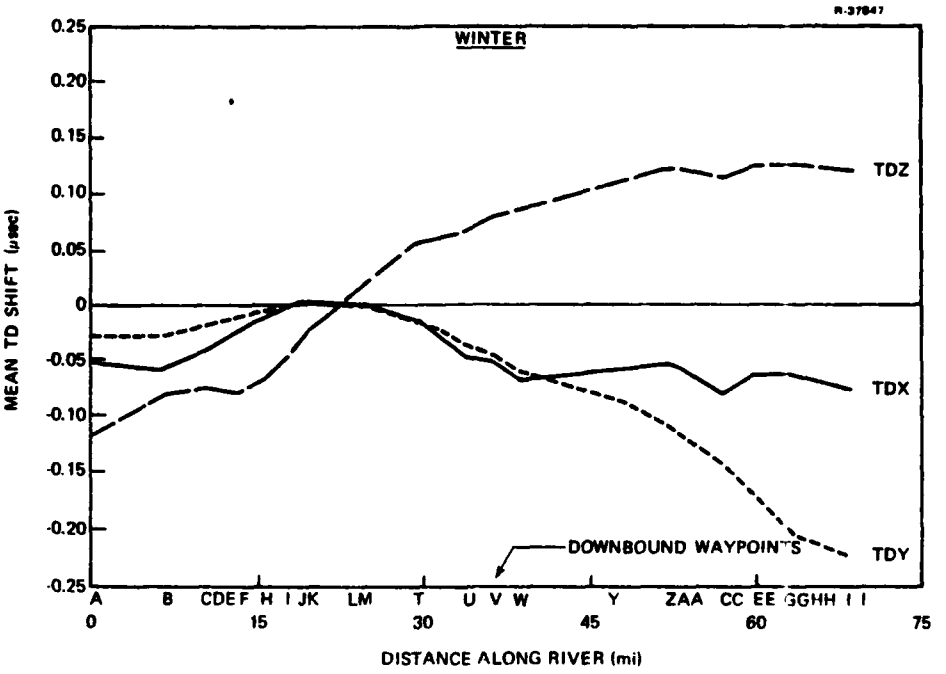

Figure 3.3-1 Predicted Mean TD Shifts in Winter at Downbound Waypoints

The results indicate that mean TD shifts do not exceed 5 nsec for spring, summer and fall, but can exceed 200 nsec (with an average of 61 nsec) for winter. This behavior is attributed to the following:

- Phase delay sensitivity to n (0.001 nsec/μsec per change of 10^{-6} in n) and to α (0.005 nsec/μsec per change of 0.01 in α) is insignificant compared with sensitivity to σ_c.
- The relative change in phase delay for a change in conductivity from 0.0047 to 0.0024 mho/m is approximately 0.7 nsec/μsec.
- Mean conductivities for spring, summer and fall have been assumed to equal the estimated conductivity for September 1977 data collection. Therfore, only changes in n and α contribute to mean TD shifts for these seasons.

- Resulting mean winter TD shifts are a direct consequence of the assumed decrease in mean conductivity between September 1977 and winter.

Although the specific mean TD shifts predicted by this study can only be as reliable as the assumed mean parameter variations, two conclusions can be drawn with some confidence. First, changes in refractive index and the parameter α do not contribute more than 20 nsec to TD variations. Second, there is a potential for changes in ground conductivity to produce significant TD variations.

An additional observation can be made upon inspection of Fig. 3.3-1. There is no mean shift in TDs at the SAM (located near waypoint L), but the magnitude of the shift increases as the differential range from SAM (magnitude of the difference between waypoint TD and SAM TD) increases. Although the shift does not increase monotonically with distance along the river from SAM, the greatest shift tends to be near the extreme waypoints.

3.3.2 Random Seasonal TD Variations

In any particular year, the actual seasonal cycle of a propagation parameter may differ significantly from the mean cycle, which is the average over many years. The year-to-year parameter variations are referred to here as random variations because they cannot be identified a priori. There may also be variations within a season in a particular year, but the available data do not permit the statistics of these variations to be determined. Expected random (1σ) TD variations corresponding to the assumed random (1σ) parameter variations of Table 3.3-1, are illustrated for summer and winter in Figs. 3.3-2 and 3.3-3. Random TD variations for

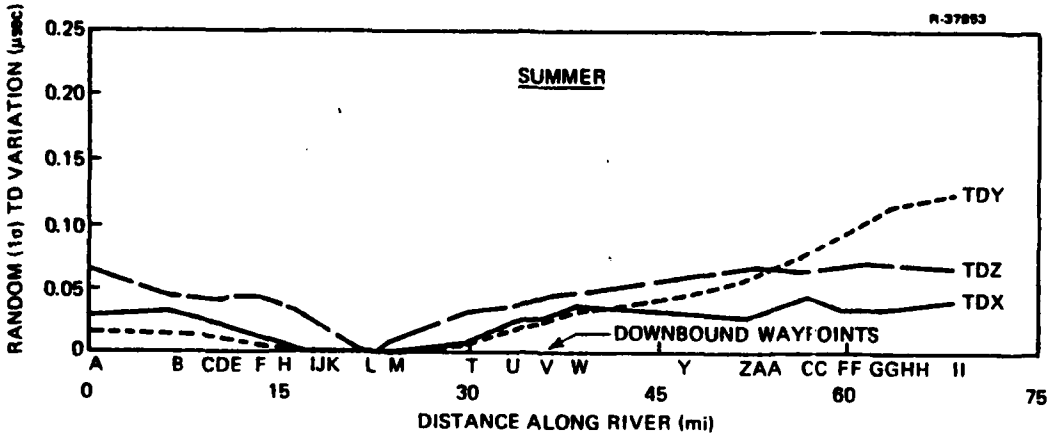

Figure 3.3-2 Predicted Random TD Variations in Summer at Downbound Waypoints

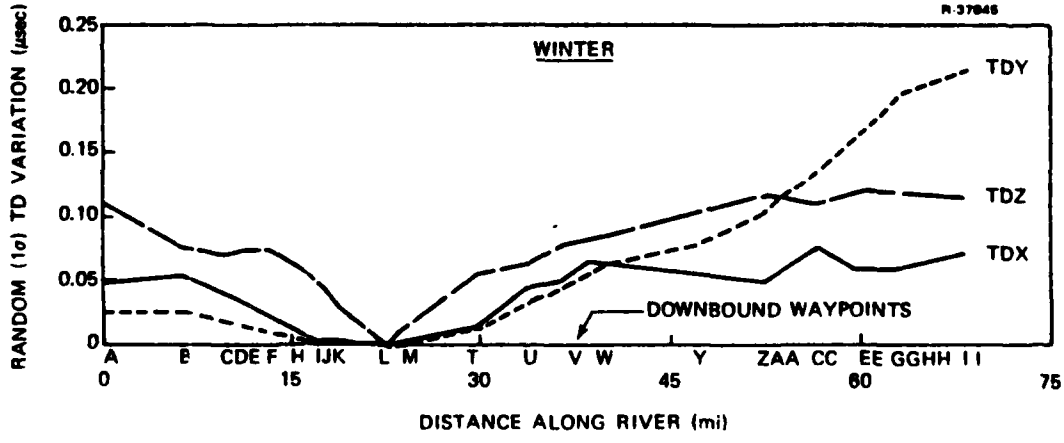

Figure 3.3-3 Predicted Random TD Variations in Winter at Downbound Waypoints

all seasons and all waypoints are tabulated in Appendix C (Tables C-1 to C-4).

Because variations in n and α contribute little to TD variations (see Section 3.3.1) and because random conductivity variations for spring, summer and fall are assumed

equal, random TD variations are essentially the same for these seasons (approximately 125 nsec maximum and 50 nsec rms). Random TD variations for winter increase to approximately 200 nsec maximum and 75 nsec rms, due to the assumed increase in the 1σ conductivity factor (defined in Section 3.2.3) from 1.5 in other seasons to 2.0 in winter. On comparing Figs. 3.3-1 and 3.3-3, it is observed that, in winter, the mean TD shifts approximately equal the random TD variations. If a priori compensation for mean TD shifts were applied to the calibrated grid, then random temporal grid instability would remain. If the random component of grid instability varys slowly over the year, then compensation may be determined and applied periodically. If the variations are rapid, however, then some form of real-time compensation would be required. The results presented in this section are based on reasonable estimates of conductivity variations and are subject to revision if better conductivity data becomes available.

3.3.3 Comparison With Observed Variations

Subsequent to collecting data during September 1977 for grid calibration, the U.S. Coast Guard revisited 10 of the data collection sites as many as four times between November 1977 and March 1978. Figure 3.3-4 shows site TDs (after editing outliers and averaging an ensemble of 0.5 hr data collection intervals) relative to TDs predicted by the RB model, for the 10 revisited sites (see Fig. 3.3-5) and all five data collection periods. This chart reveals temporal variations in site TDs, as well as differences (residuals) between observed TDs and the calibrated grid.

The residuals for September 1977 (data collection period A) may include unmodelled spatial details (local

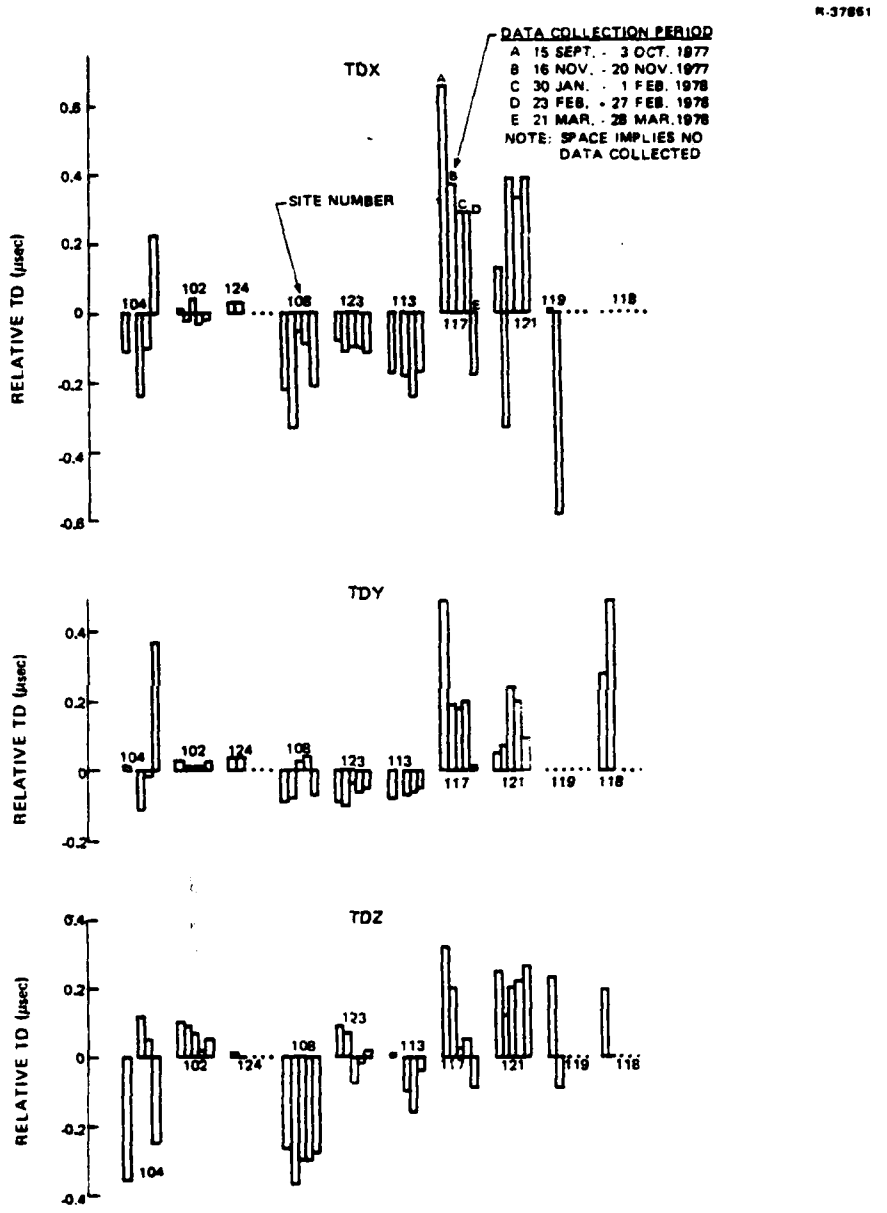

Figure 3.3-4 TD Data Relative to Calibrated Grid for Five Data Collection Periods

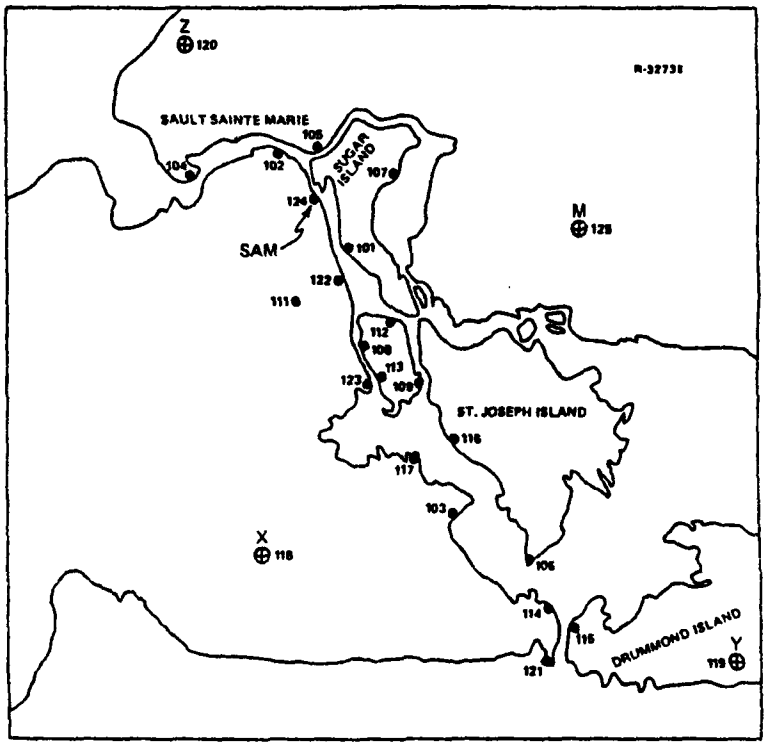

Figure 3.3-5 Data Collection Sites

warpages), temporal grid instability over the 18 days of data collection, and measurement errors. Temporal variations over 18 days are expected to be small based on observed variations in refractive index and the parameter α and on reasonable variations in conductivity. (However, some temporal variation may be caused by weather effects such as rain or the passage of weather fronts.) Significant local warpages apparently exist, as indicated by nearly constant residuals for all data collection periods at some sites, such as 113 (TDX) and 108 (TDZ). The relative importance of temporal variations, local warpages and measurement errors cannot be determined from the present data set. It is conceivable that calibration residuals would be smaller than those shown in Fig. 3.3-4 if the data did not include temporal variations and measurement errors.

The TD variations between data collection periods revealed by Fig. 3.3-4 are of particular interest to this study. Site TDs corresponding to the data collection periods cannot be predicted without first relating conductivity to physical ground parameters for the periods. However, a comparison of observed variations to those predicted in Sections 3.3.1 and 3.3.2 reveals the following:

- SAM TDs (site 124) vary less than 10 nsec
- TD variations at sites 102, 123, and 113 are under 100 nsec peak-to-peak and may be explainable by expected parameter variations
- TD variations at the other six sites are unusually large (850 nsec maximum and 300 nsec average) and cannot be easily explained by assumed parameter variations
- The average peak-to-peak TD variation over all revisited sites is 240 nsec.*

The unexplained temporal variations may be caused by something other than propagation effects such as differences in the receiving antenna ground plane during the separate data collection periods, or unmodelled weather effects. It could also be that some sites such as those identified as anomalous in Ref. 1 (namely 104, 108, and 117) may exhibit localized temporal variations. The large variations at sites 118 (X station) and 119 (Y station) were very likely caused by a change in the grounding environment associated with moving the receiving antenna from the top of the transmitting tower (in September) to the earth (in November). Although observed TD variations apparently cannot be explained by expected variations

*Editing of selected data at sites 104, 117, 118, 119 and 121, which may be anomalous, reduces the average to 100 nsec.

in the propagation parameters considered herein, this should be substantiated by a long-term signal monitoring effort.

3.4 POSITION ERRORS AT WAYPOINTS

In Section 3.3, seasonal statistics were determined for the component of TD error caused by changes in the propagation parameters. These results are employed in this section to predict user position errors at river waypoints using the transformation equations given in Appendix B.

If the calibrated grid is not compensated for mean winter TD shifts (see Section 3.3.1), then a Loran-C user employing the grid in winter is expected to experience a deterministic (mean) position offset. The magnitude and bearing of the mean position errors at the waypoints are tabulated in Appendix C (Table C-5) for the triad of transmitter stations which yields minimum error with the calibrated grid model. Although the magnitude of the mean winter offset has an average value of approximately 60 ft (over all waypoints), a correction table could be employed by the user to compensate for this offset in the winter TD grid.

In addition to mean TD shifts, random seasonal grid instability (see Section 3.3.2) also contributes to position error. This contribution is plotted in Fig. 3.4-1 for summer* and for winter at the downbound waypoints for the same station triad as used to evaluate the calibrated grid in Ref. 1 (see Table C-5). Random position errors are tabulated in Appendix C (Table C-6) for all station triads. This random component

*Random propagation errors for spring and fall are essentially the same as for summer.

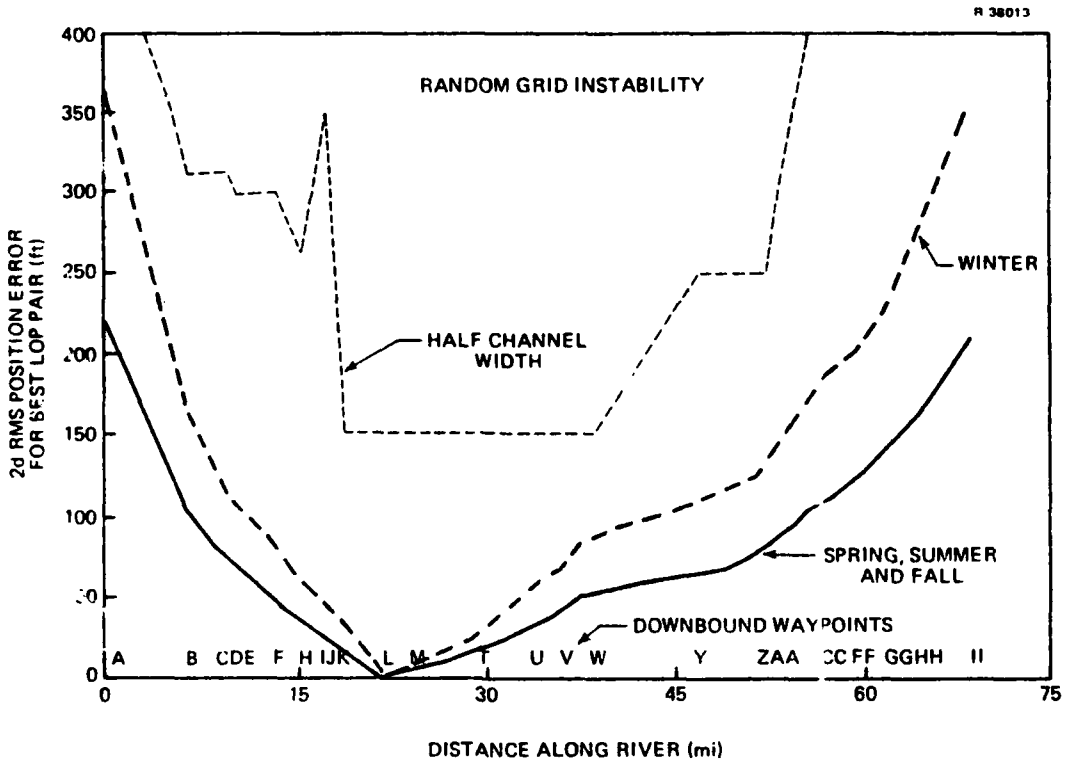

Figure 3.4-1 Component of 2d rms Position Error at Downbound Waypoints Due to Random Seasonal Grid Instability

of grid instability is interpreted as the variability in the grid from one year to another during the specified season. The variability over a given season is difficult to assess since historical meteorological data are only available as monthly averages and conductivity data are not available. The increase in position error at the extremes of the river is due to the combined effect of SAM and GDOP*. Note that even if the RB model provides an error-free prediction of the grid which existed during September 1977 data collection, there would still be 2d rms position errors (Eq. B-6) of 75 ft (rms over all waypoints) in spring, summer and fall and 130 ft in

*Geometric Dilution of Precision

winter from one year to another. However, it should also be noted that this predicted variation in the grid is due primarily to predicted variations in conductivity from year to year. The practicality of compensating (by the user) for these variations in the grid depends on the frequency of the fluctuations. For example, if the variation is slow, it may be possible to provide a simple first-order grid compensation algorithm in the user equipment which is valid for a month or even the entire season. The result would be to reduce the predicted errors due to the modelled random effects.

In actuality, the RB model does not predict the September 1977 grid exactly and other contributors to position error must be considered. Equation 2.2-2 expresses the total TD error invoked when using the RB model to predict the true TD (the grid measured in the absence of noise). The total error includes three components:

- Residual grid prediction error (model calibration error) -- error due to an inability to determine exactly the coefficients of the RB model with a finite amount of noisy data
- Local warpage -- unmodelled spatial details which do not change with time
- Temporal grid instability -- variations due to changing propagation conditions (seasonal, diurnal, and weather front passage effects).

If position is established at a waypoint by employing noiseless TD measurements and the calibrated RB grid, then the total position error (relative to the actual waypoint) includes a component due to each of the above components of TD error. In Fig. 3.4-2 the residual grid prediction (position) error is reproduced from Ref. 1. This curve is a theoretical

lower bound on the expected 2d rms position error and can only be approached if both local warpage and temporal grid instability are negligible. It should be kept in mind that this bound is a characteristic of the particular spatial-area model structure chosen (range and bearing polynomial) and of the quality and quantity of the particular data used for calibration.

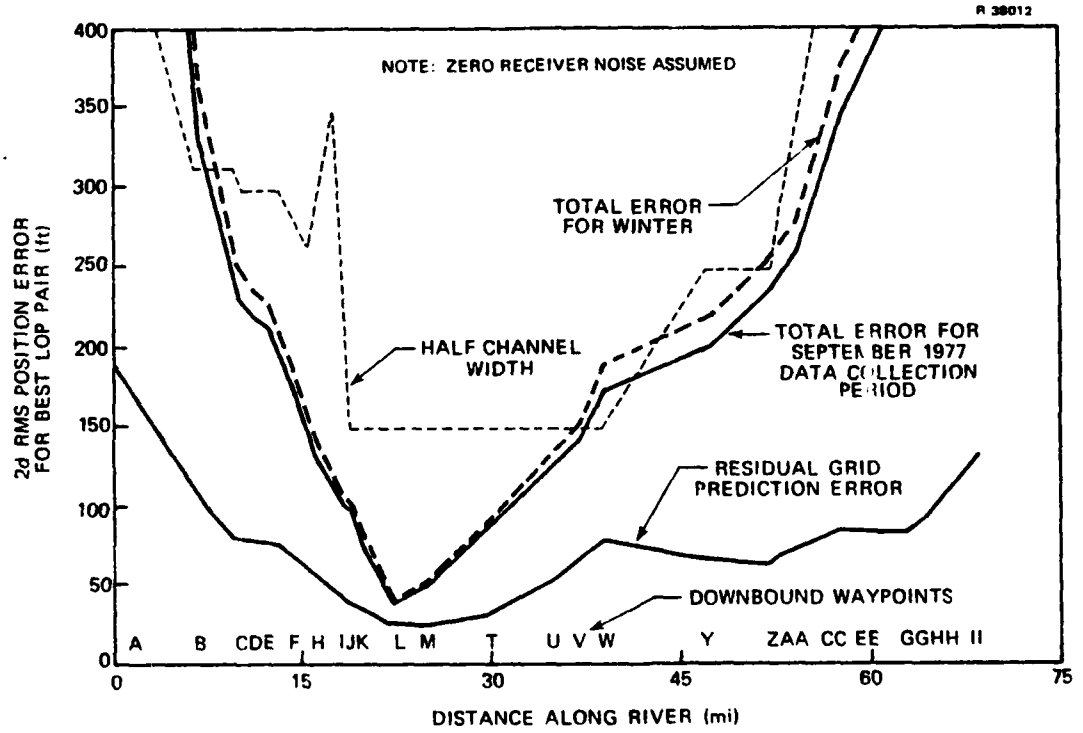

Figure 3 4-2 Residual Grid Prediction Errors and Total September 1977 and Winter Errors at Downbound Waypoints

An upper bound on the expected 2d rms position error at the waypoints for the September 1977 data collection period is shown in Ref. 1 and reproduced in Fig. 3.4-2. This bound was arrived at on an ad hoc basis in Ref. 1 in an attempt to characterize the observed site-to-site variability of the September 1977 data relative to the RB model. Local warpage

and temporal grid instability, as well as measurement uncertainties (e.g., potential site-to-site ground plane differences), all contribute to the observed site-to-site variability in the data. Additional data collected since the September 1977 data collection period are not sufficient to allow this bound to be changed at this time. A Loran-C user, employing the calibrated grid on the St. Marys River during the fall of another year, will still encounter local warpage due to any unmodelled spatial details of signal propagation. However, the user would probably not experience the same measurement problems or short-term temporal effects which may have occurred during September 1977 data collection. On the other hand, the contribution of fall grid instability (from year to year, as discussed in this report) to user position error is expected to be greater than the contribution of grid instability over the 18 days of September 1977 data collection. Because the relative contribution of local warpage, temporal grid instability and measurement error to the predicted September 1977 position errors is not known, the total user position error during another fall cannot be determined exactly.

If the predicted position errors for September 1977 data collection are assumed to be representative of errors for any fall, however, then these errors can serve as a baseline for predicting winter position errors. The total winter position errors shown in Fig. 3.4-2 (and tabulated in Table C-7) were determined by employing this fall baseline along with the incremental change in predicted position errors between fall and winter due to random grid instability (shown in Fig. 3.4-1). The total winter position errors should be interpreted as an expected upper bound on the predicted position error for a Loran-C user navigating the St. Marys River in any season. It is evident from Fig. 3.4-2 that the additional contribution of winter grid instability to position

error is small when combined in a root-sum-square sense with position errors for the September 1977 data collection period predicted in Ref. 1. The 2d rms position error (rms over all waypoints) increases from 290 ft for September 1977 data collection to 310 ft for winter.

When interpreting the total position errors predicted herein, it must be remembered that the observed site-to-site variability in the 1977 data, relative to the RB model, was the basis for the mathematical model used to predict the associated total position error at the waypoints. If a major component of this observed site-to-site variability is due to local warpage effects which are constant with time, it may be possible to reduce these errors (e.g., by using force-fit techniques) and thereby reduce the total error at the waypoints. Because the resulting total error would be smaller, the relative change between fall and winter would become more significant. A comprehensive data monitoring effort should permit the major contributors to total grid error to be isolated and thereby allow better predictions of position error to be determined.

4. CONCLUSIONS AND RECOMMENDATIONS

4.1 CONCLUSIONS

This study has predicted the impact of expected seasonal variations in propagation parameters on the stability of the St. Marys River Loran-C time difference grid. Sensitivity of the grid to the important propagation parameters -- surface refractive index n, the parameter α associated with refractive index gradient, and ground conductivity σ_c -- follows from classical propagation theory. TD variations, corresponding to estimates of seasonal parameter variations, were computed and compared with TD variations embodied in U.S. Coast Guard data. Position errors at river waypoints were then determined from the TD variations in order to assess the impact of temporal grid instability on a Loran-C user.

During the study, it was found that seasonal variations in the parameters n and α can be characterized statistically from historical meteorological data recorded at the National Weather Service Station at Sault Sainte Marie, Michigan. However, characterization of the ground conductivity is complicated by the heterogeneity of the region and by the inadequacy of published data. The following seasonal analysis results are based on best available estimates of seasonal parameter variations:

- The effect of variations in n and α on grid instability is less than 20 nsec at all waypoints
- The mean difference between TDs in spring, summer, and fall, and TDs in winter is 60 nsec averaged over all waypoints

- Random (1σ) TD variations (about the mean) due to assumed conductivity variations are approximately 45 nsec rms for spring, summer and fall and 75 nsec rms for winter.

The predictions of grid instability computed in this study cannot explain the TD variations observed at most data collection sites (240 nsec peak-to-peak, averaged over all revisited sites). This conclusion is based upon theoretical models and expected propagation parameter variations, and should be validated by a more comprehensive data collection effort.

Predicted position errors at the waypoints have been computed corresponding to both mean seasonal TD shifts and random (1σ) TD variations. The deterministic (mean) position offsets corresponding to mean winter TD shifts average 60 ft in magnitude but can be removed by grid compensation. Random position errors (Fig. 3.4-1) cannot be removed by a priori grid compensation, and add to position errors due to grid prediction (calibration) and local warpage (unmodelled spatial details). If the RB model were capable of perfectly representing the grid which existed during September 1977, then estimated random seasonal grid instability would still contribute an average (over all waypoints) of 75 ft 2d rms position error in spring, summer and fall and 130 ft in winter. An average total 2d rms position error of 290 ft associated with the upper bound on position error during September 1977 data collection (Ref. 1 and Fig. 3.4-2), and assumed to be representative of conditions occurring during any fall, increases to 310 ft for winter. It should be kept in mind, however, that the predicted waypoint position errors in Ref. 1 may include the effect of site-to-site measurement errors (e.g., antenna ground plane differences) which cannot be identified from the available data and would not be experienced by a user at the

waypoints. Also, there is some evidence from the revisited site data that local warpage may be a significant contributor to the observed site-to-site grid prediction errors. Calibration of these local warpages (assuming they do not change with time) would also reduce the predicted waypoint position errors. Finally, ground conductivity variations constitute the major contribution to predicted seasonal grid instability. If these variations in conductivity are relatively slow, it may be possible to provide compensation in the user equipment which is valid for a month or an entire season.

4.2 RECOMMENDATIONS

In order to quantify the apparent grid instability observed in the St. Marys River Loran-C data, it is recommended that a comprehensive data collection effort be initiated. Preliminary considerations suggest the following approach:

- Isolate receiver/environment instabilities
- Collect long-term data at strategically-located sites
- Continue collecting short-term seasonal data at other translocation sites
- Analyze long-term and short-term data to identify grid instability.

Each of the above is expanded upon below.

It is first necessary to determine whether or not the data collection procedure itself has contributed to the apparent instability. The adequacy of the receiving antenna ground plane should be determined, especially as influenced by site environment, e.g., 1-2 m deep snow cover. Furthermore, the

potential impact of precipitation and fog (at the antenna) on the phase of the received signal should be tested.

It is recommended that long-term time of arrival (TOA) data be collected continuously (≈ 15-minute averages) for several months at a few strategically-located sites, to be determined by covariance simulation. TOA data is especially useful in isolating those propagation effects which are not experienced by the entire chain. In addition to continuous long-term data, it is suggested that four-hour TD data be collected, at least seasonally, at translocation sites where long-term data are not collected. These data, in combination with long-term data, would permit the determination of the spatial extent of any observed instability.

In order to interpret the data, the following additional information would be valuable:

- SAM-applied local phase adjustments
- Signal to noise ratio, ECD, and receiver settings
- Meteorological data.

Analysis of data from an intensive collection program, such as the above, should reveal the extent of temporal grid instability and its relative impact on the operational status of the St. Marys River Loran-C chain. If the apparent grid instability is substantiated by this data analysis, the data should be used to establish the feasibility of compensation algorithms for temporal grid instability.

APPENDIX A
COMPUTATION OF TD VARIATIONS

The sensitivity equations developed in Sections 2.3 and 2.4 can be employed to compute mean TD shifts (Section 3.3.1) and random (1σ) TD variations (Section 3.3.2) at any location in the St. Marys River Loran-C signal coverage area. These equations are summarized below.

Mean TD shifts follow from Eqs. 2.3-2, 2.3-6, 2.3-7, 2.4-2, and 2.4-3. The mean shift (expected value, $\mathcal{E}$) in TD_i (μsec) from September 1977 (calibration) to another time (season) is

$$\mathcal{E}(\Delta TD_i) = \mathcal{E}(TD_i)_{\text{season}} - \mathcal{E}(TD_i)_{\text{calibration}} \qquad \text{(A-1)}$$

where mean TDs are computed from

$$\mathcal{E}(TD_i) = \left[(T_i - T_m) + (SF_i - SF_m)\right] - \left[(T_i' - T_m') + (SF_i' - SF_m')\right] + TD_i^o \qquad \text{(A-2)}$$

Note that TD_i^o, the reference TD for SAM, does not influence mean TD shifts. In Eq. A-2, primary and secondary phase delays are denoted by T and SF, respectively; unprimed phase delays are between the transmitting stations and the user, while primed (') phase delays are between the stations and SAM; and the secondary and master stations are distinguished by subscripts i and m. Phase delays are computed from mean propagation parameters $\bar{n}$, $\bar{\alpha}$, and $\bar{\sigma}_c$ (for calibration or season) by

$$T = \left(\frac{\bar{n}}{c}\right) R \quad (\mu\text{sec}) \qquad \text{(A-3)}$$

$$SF = \sum_{k=-2}^{2} \sum_{\ell=-1}^{1} A_{k\ell} \, (\ln \bar{\sigma}_c)^{\ell} \, T^k + 0.0005 \, (\bar{\alpha}-0.75) \, T \qquad \text{(A-4)}$$

where

c = 983.5690892 ft/μsec

$A_{k\ell}$ = coefficients from Table 2.3-1

R = path distance (ft) from a station to the user or SAM.

Note that Eq. A-4 is only valid for mean conductivities 0.001 to 0.01 mho/m.

Random (1σ) TD variations follow from Eqs. 2.4-2, 2.4-4, 2.4-5, and 2.4-6. The 1σ TD variation, $\Delta\tilde{TD}_i$, corresponding to 1σ variations of $\Delta\tilde{n}$, $\Delta\tilde{\alpha}$, and $\Delta\tilde{\xi}$ (where $\xi = \ell n \, \sigma_c$) is

$$\Delta\tilde{TD}_i = \left[(h_n^i \, \Delta\tilde{n})^2 + (h_\alpha^i \, \Delta\tilde{\alpha})^2 + (h_\xi^i \, \Delta\tilde{\xi})^2 \right]^{1/2} \qquad \text{(A-5)}$$

where the required sensitivity coefficients are defined below:

$$h_n^i = \left[(T_i - T_m) - (T_i' - T_m') \right] \qquad \text{(A-6)}$$

$$h_\alpha^i = 0.0005 \left[(T_i - T_m) - (T_i' - T_m') \right] \qquad \text{(A-7)}$$

$$h_\xi^i = -0.039 \left[(T_i^a - T_m^a) - (T_i'^a - T_m'^a) \right] \qquad \text{(A-8)}$$

$$a = 0.47 \qquad \text{(A-9)}$$

Note that Eq. A-5 permits the contribution of each parameter variation to be isolated.

APPENDIX B
COMPUTATION OF POSITION ERRORS

Equations for transforming TD errors to position errors, similar to equations developed in Ref. 1, are presented below. If a hyperbolic position fix is obtained using secondary stations i and j, then the relationship between TD errors (ΔTD_i and ΔTD_j) and north (ΔN) and east (ΔE) position errors is

$$\begin{bmatrix} \Delta N \\ \Delta E \end{bmatrix} = H_u \begin{bmatrix} \Delta TD_i \\ \Delta TD_j \end{bmatrix} \qquad \text{(B-1)}$$

where H_u is a 2x2 matrix which depends on station and user locations and is related to the crossing angle between the hyperbolic lines of position. The mean (expected value, $\mathcal{E}$ position error corresponding to mean TD shifts (see Appendix A, Eq. A-1) is thus given by

$$\begin{bmatrix} \mathcal{E}(\Delta N) \\ \mathcal{E}(\Delta E) \end{bmatrix} = H_u \begin{bmatrix} \mathcal{E}(\Delta TD_i) \\ \mathcal{E}(\Delta TD_j) \end{bmatrix} \qquad \text{(B-2)}$$

and may be interpreted as a vector with magnitude and bearing.

In addition to mean TD shifts, there are random position errors due to random variations in propagation parameters as well as due to residual grid prediction error, local warpage, and user measurement noise. Random position errors are represented by the covariance matrix of the position error vector (ΔN, ΔE). The total position error covariance for zero measurement noise is computed (see Ref. 17) by

$$P = H_u \left[R_{rg} + R_{\ell w} + R_{tg} \right] H_u^T \qquad \text{(B-3)}$$

where the superscript T denotes transpose and

R_{rg} = covariance of residual grid prediction error

$R_{\ell w}$ = covariance of local warpage error

R_{tg} = covariance of temporal grid instability.

R_{rg} is related to the error covariance of the RB model coefficients, and depends only on the quantity and quality of calibration data, as detailed in Ref. 1. $R_{\ell w}$ is based on assumed local warpage, as described in Section 3.4. The covariance of temporal grid instability is related to 1σ variations ($\tilde{\Delta n}$, $\tilde{\Delta\alpha}$, $\tilde{\Delta\xi}$) in the propagation parameters by

$$R_{tg} = H_{tg} \begin{bmatrix} (\tilde{\Delta n})^2 & 0 & 0 \\ 0 & (\tilde{\Delta\alpha})^2 & 0 \\ 0 & 0 & (\tilde{\Delta\xi})^2 \end{bmatrix} H_{tg}^T \qquad \text{(B-4)}$$

where the matrix which relates parameter variations to TD variations is

$$H_{tg} = \begin{bmatrix} h_n^i & h_\alpha^i & h_\xi^i \\ h_n^j & h_\alpha^j & h_\xi^j \end{bmatrix} \qquad \text{(B-5)}$$

and the matrix elements are defined in Appendix A (Eqs. A-6 to A-8).

The diagonal entries of P are denoted by p_N and p_E, and the error quantity in common usage by the U.S. Coast Guard (Ref. 3) is

$$\text{2d rms error} = 2\sqrt{p_N + p_E} \qquad \text{(B-6)}$$

APPENDIX C
TABLES OF TD VARIATIONS AND POSITION ERRORS

Tables C-1 to C-4 present mean TD shifts (TD for the season minus TD for September 1977) and random (1σ) TD variations at all waypoints for four seasons. Table C-5 shows the magnitude and bearing of the mean position error for winter, at all waypoints for the station combination which yields minimum error with the calibrated grid model. Table C-6 presents the component of 2d rms position error due to random seasonal grid instability, at all waypoints for all three station combinations, for summer and winter. Table C-7 presents total 2d rms position errors at all waypoints for all three station combinations, for the September 1977 data collection period and for winter.

TABLE C-1

PREDICTED TD VARIATIONS AT WAYPOINTS FOR SPRING

T-2559

WAYPOINT	MEAN TD SHIFT (μsec)			RANDOM (1σ) TD VARIATION (μsec)		
	TDX	TDY	TDZ	TDX	TDY	TDZ
A	-0.001	0.000	-0.001	0.028	0.015	0.065
B	-0.001	0.000	-0.001	0.032	0.015	0.044
C	-0.001	0.000	-0.001	0.024	0.011	0.041
D	0.000	0.000	-0.001	0.023	0.011	0.041
E	0.000	0.000	-0.001	0.020	0.009	0.043
F	0.000	0.000	-0.001	0.013	0.006	0.043
H	0.000	0.000	-0.001	0.007	0.003	0.036
I	0.000	0.000	0.000	0.001	0.001	0.027
J	0.000	0.000	0.000	0.001	0.000	0.024
K	0.000	0.000	0.000	0.002	0.001	0.016
L	0.000	0.000	0.000	0.001	0.000	0.000
M	0.000	0.000	0.000	0.001	0.000	0.009
N	0.000	0.000	0.000	0.001	0.000	0.011
O	0.000	0.000	0.000	0.002	0.002	0.021
P	0.000	0.000	0.001	0.007	0.009	0.041
Q	0.000	0.000	0.001	0.002	0.008	0.056
R	0.000	-0.001	0.001	0.010	0.020	0.057
S	0.000	-0.001	0.001	0.010	0.022	0.060
T	-0.000	0.000	0.001	0.007	0.007	0.031
U	-0.001	-0.001	0.001	0.025	0.019	0.037
V	-0.001	-0.001	0.001	0.028	0.024	0.045
W	-0.001	-0.001	0.001	0.037	0.032	0.048
X	-0.001	-0.001	0.001	0.031	0.036	0.056
Y	-0.001	-0.001	0.001	0.033	0.045	0.061
Z	-0.001	-0.001	0.001	0.029	0.059	0.068
AA	-0.001	-0.001	0.001	0.030	0.064	0.068
BB	-0.001	-0.002	0.001	0.042	0.076	0.064
CC	-0.001	-0.002	0.001	0.044	0.078	0.064
DD	-0.001	-0.002	0.001	0.042	0.080	0.065
EE	-0.001	-0.002	0.002	0.034	0.094	0.069
FF	-0.001	-0.002	0.002	0.029	0.106	0.072
GG	-0.001	-0.002	0.002	0.034	0.110	0.070
HH	-0.001	-0.003	0.002	0.036	0.114	0.069
II	-0.001	-0.003	0.002	0.042	0.123	0.066

TABLE C-2

PREDICTED TD VARIATIONS AT WAYPOINTS FOR SUMMER

T-2560

WAYPOINT	MEAN TD SHIFT (μsec)			RANDOM (1σ) TD VARIATION (μsec)		
	TDX	TDY	TDZ	TDX	TDY	TDZ
A	0.000	0.000	0.000	0.028	0.015	0.065
B	0.000	0.000	0.000	0.032	0.015	0.044
C	0.000	0.000	0.000	0.024	0.011	0.041
D	0.000	0.000	0.000	0.023	0.011	0.041
E	0.000	0.000	0.000	0.020	0.009	0.043
F	0.000	0.000	0.000	0.013	0.005	0.043
H	0.000	0.000	0.000	0.007	0.003	0.036
I	0.000	0.000	0.000	0.001	0.001	0.027
J	0.000	0.000	0.000	0.001	0.000	0.024
K	0.000	0.000	0.000	0.002	0.001	0.016
L	0.000	0.000	0.000	0.001	0.000	0.000
M	0.000	0.000	0.000	0.001	0.000	0.009
N	0.000	0.000	0.000	0.001	0.000	0.011
O	0.000	0.000	0.000	0.002	0.002	0.021
P	0.000	0.000	0.000	0.007	0.003	0.041
Q	0.000	0.000	0.000	0.002	0.003	0.056
R	0.000	0.000	0.000	0.010	0.020	0.057
S	0.000	0.000	0.000	0.019	0.023	0.060
T	0.000	0.000	0.000	0.008	0.007	0.032
U	0.000	0.000	0.000	0.025	0.019	0.037
V	0.000	0.000	0.000	0.028	0.024	0.045
W	0.000	0.000	0.000	0.037	0.032	0.048
X	0.000	0.000	0.000	0.031	0.036	0.056
Y	0.000	0.000	0.000	0.033	0.045	0.061
Z	0.000	-0.001	0.001	0.029	0.059	0.068
AA	0.000	-0.001	0.001	0.030	0.064	0.068
BB	0.000	-0.001	0.001	0.042	0.076	0.064
CC	0.000	-0.001	0.001	0.044	0.073	0.064
DD	0.000	-0.001	0.001	0.042	0.081	0.065
EE	0.000	-0.001	0.001	0.034	0.09-	0.069
FF	0.000	-0.001	0.001	0.029	0.10(	0.072
GG	0.000	-0.001	0.001	0.034	0.11(	0.070
HH	0.000	-0.001	0.001	0.036	0.11-	0.069
II	0.000	-0.001	0.001	0.042	0.12-	0.066

TABLE C-3

PREDICTED TD VARIATIONS AT WAYPOINTS FOR FALL

T-2561

WAYPOINT	MEAN TD SHIFT (μsec)			RANDOM (1σ) TD VARIATION (μsec)		
	TDX	TDY	TDZ	TDX	TDY	TDZ
A	0.000	0.000	0.000	0.028	0.015	0.065
B	0.000	0.000	0.000	0.032	0.015	0.044
C	0.000	0.000	0.000	0.024	0.011	0.041
D	0.000	0.000	0.000	0.023	0.011	0.041
E	0.000	0.000	0.000	0.020	0.009	0.043
F	0.000	0.000	0.000	0.013	0.006	0.043
H	0.000	0.000	0.000	0.007	0.003	0.036
I	0.000	0.000	0.000	0.001	0.001	0.027
J	0.000	0.000	0.000	0.001	0.000	0.024
K	0.000	0.000	0.000	0.002	0.001	0.016
L	0.000	0.000	0.000	0.001	0.000	0.000
M	0.000	0.000	0.000	0.001	0.000	0.009
N	0.000	0.000	0.000	0.001	0.000	0.011
O	0.000	0.000	0.000	0.002	0.002	0.021
P	0.000	0.000	0.000	0.007	0.009	0.041
Q	0.000	0.000	0.000	0.002	0.009	0.056
R	0.000	0.000	0.000	0.010	0.020	0.057
S	0.000	0.000	0.000	0.010	0.022	0.060
T	0.000	0.000	0.000	0.008	0.007	0.032
U	0.000	0.000	0.000	0.025	0.019	0.037
V	0.000	0.000	0.000	0.028	0.024	0.045
W	0.000	0.000	0.000	0.027	0.033	0.048
X	0.000	0.000	0.000	0.031	0.036	0.056
Y	0.000	0.000	0.000	0.033	0.045	0.061
Z	0.000	0.000	0.000	0.029	0.059	0.068
AA	0.000	0.000	0.000	0.030	0.064	0.068
BB	0.000	0.000	0.000	0.042	0.076	0.065
CC	0.000	0.000	0.000	0.044	0.078	0.064
DD	0.000	0.000	0.000	0.042	0.080	0.065
EE	0.000	-0.001	0.000	0.034	0.094	0.069
FF	0.000	-0.001	0.000	0.029	0.106	0.072
GG	0.000	-0.001	0.000	0.034	0.110	0.070
HH	0.000	-0.001	0.000	0.036	0.115	0.069
II	0.000	-0.001	0.000	0.042	0.124	0.066

TABLE C-4

PREDICTED TD VARIATIONS AT WAYPOINTS FOR WINTER

T-2562

WAYPOINT	MEAN TD SHIFT (μsec)			RANDOM (1σ) TD VARIATION (μsec)		
	TDX	TDY	TDZ	TDX	TDY	TDZ
A	-0.051	-0.027	-0.117	0.048	0.026	0.111
B	-0.057	-0.027	-0.079	0.054	0.026	0.076
C	-0.044	-0.020	-0.074	0.042	0.019	0.071
D	-0.041	-0.019	-0.074	0.039	0.018	0.071
E	-0.036	-0.017	-0.078	0.034	0.016	0.074
F	-0.023	-0.010	-0.077	0.021	0.010	0.074
H	-0.012	-0.005	-0.065	0.011	0.005	0.062
I	-0.002	-0.001	-0.048	0.002	0.001	0.046
J	-0.001	0.000	-0.042	0.001	0.000	0.040
K	0.003	0.002	-0.029	0.003	0.002	0.028
L	0.001	0.001	0.001	0.001	0.001	0.001
M	0.002	0.000	0.017	0.002	0.000	0.016
N	0.002	0.000	0.020	0.002	0.000	0.019
O	-0.004	-0.004	0.038	0.004	0.004	0.036
P	-0.012	-0.016	0.073	0.011	0.015	0.069
Q	0.004	-0.015	0.100	0.004	0.014	0.095
R	-0.019	-0.035	0.103	0.018	0.034	0.098
S	-0.019	-0.040	0.108	0.018	0.038	0.103
T	-0.013	-0.013	0.056	0.013	0.012	0.054
U	-0.045	-0.034	0.066	0.043	0.032	0.063
V	-0.050	-0.044	0.080	0.048	0.042	0.076
W	-0.066	-0.058	0.085	0.063	0.055	0.081
X	-0.055	-0.065	0.100	0.053	0.062	0.095
Y	-0.059	-0.081	0.108	0.056	0.077	0.103
Z	-0.052	-0.106	0.121	0.049	0.101	0.115
AA	-0.055	-0.114	0.121	0.052	0.108	0.116
BB	-0.075	-0.135	0.116	0.071	0.129	0.110
CC	-0.079	-0.140	0.114	0.075	0.133	0.109
DD	-0.076	-0.143	0.116	0.072	0.136	0.111
EE	-0.062	-0.168	0.124	0.059	0.160	0.118
FF	-0.052	-0.191	0.129	0.050	0.182	0.123
GG	-0.061	-0.197	0.125	0.058	0.187	0.119
HH	-0.064	-0.205	0.124	0.061	0.195	0.118
II	-0.074	-0.221	0.119	0.071	0.211	0.113

TABLE C-5

PREDICTED MEAN POSITION ERRORS AT WAYPOINTS FOR WINTER[†]
DUE ONLY TO VARIATIONS IN PROPAGATION PARAMETERS

T-2563

WAYPOINT	BEST TRIAD	MEAN WINTER POSITION ERROR	
		MAGNITUDE (ft)	BEARING FROM NORTH (deg)
A	MXZ	200	-66
B	MXZ	92	-85
C	MXZ	64	-82
D	MXZ	60	-81
E	MXZ	58	-77
F	MXZ	45	-66
H	MXZ	34	-55
I	MXZ	26	-40
J	MXZ	23	-38
K	MXZ	18	-26
L	MXZ	1	45
M	MXZ	9	137
N	MXZ	12	138
O	MXZ	22	125
P	MXY	18	159
Q	MXY	22	133
R	MXY	30	153
S	MXY	33	151
T	MXY	14	170
U	MXY	31	-176
V	MXY	36	178
W	MXY	46	179
X	MXY	47	171
Y	MXY	56	168
Z	MXY	67	162
AA	MXY	72	163
BB	MXY	92	171
CC	MXY	97	172
DD	MXY	98	171
EE	MXY	107	163
FF	MXY	116	158
GG	MXY	129	162
HH	MXY	142	163
II	MXY	188	166

[†]Mean position errors for spring, summer and fall are less than 1 ft.

TABLE C-6

PREDICTED COMPONENT OF 2d RMS POSITION ERROR AT WAYPOINTS DUE TO RANDOM GRID INSTABILITY, FOR SUMMER AND WINTER*

WAYPOINT	2d RMS POSITION ERROR (ft)					
	MXY		MYZ		MXZ	
	SUMMER	WINTER	SUMMER	WINTER	SUMMER	WINTER
A	67	112	301	514	223	381
B	57	96	126	215	103	175
C	41	70	86	147	71	121
D	38	65	82	139	67	115
E	34	58	78	135	64	110
F	22	37	58	100	51	86
H	12	19	41	70	38	65
I	3	4	27	47	29	49
J	2	2	24	41	26	44
K	4	6	17	29	20	34
L	1	2	1	2	1	2
M	2	4	10	17	10	18
N	3	5	12	20	13	22
O	8	13	24	41	28	48
P	20	33	51	87	62	106
Q	25	42	72	122	87	148
R	34	57	85	144	113	192
S	37	62	92	158	126	215
T	16	27	39	66	47	81
U	34	59	56	96	74	127
V	41	69	71	121	98	167
W	52	88	83	142	122	208
X	53	90	100	170	152	259
Y	62	106	118	201	197	336
Z	75	128	151	258	286	487
AA	80	136	157	268	309	528
BB	103	175	164	279	379	647
CC	108	185	165	282	397	677
DD	109	186	170	290	412	702
EE	120	204	204	348	533	909
FF	130	222	234	399	643	1097
GG	144	246	229	391	679	1157
HH	158	270	233	397	734	1252
II	210	358	239	407	895	1525

*Position errors for spring and fall are within 1 ft of those for summer.

TABLE C-7

PREDICTED TOTAL 2d RMS POSITION ERRORS AT WAYPOINTS, FOR SEPTEMBER 1977 DATA COLLECTION PERIOD AND WINTER

WAYPOINT	2d RMS POSITION ERROR (ft)					
	MXY		MYZ		MXZ	
	SEPT 1977	WINTER	SEPT 1977	WINTER	SEPT 1977	WINTER
A	850	855	998	1081	699	764
B	534	540	434	468	329	358
C	347	352	299	322	230	250
D	317	321	281	303	218	237
E	303	307	269	290	210	228
F	251	253	212	227	172	185
H	194	195	157	167	133	143
I	171	171	114	120	101	108
J	164	164	104	109	92	99
K	151	151	84	87	75	80
L	104	104	50	50	38	38
M	90	90	56	58	49	51
N	101	101	62	64	51	54
O	89	90	88	94	91	99
P	91	95	163	178	194	212
Q	109	114	228	248	272	297
R	126	134	267	291	350	383
S	136	145	293	320	393	430
T	82	85	127	138	150	164
U	126	135	179	195	231	253
V	140	151	226	246	304	333
W	173	187	268	292	379	415
X	172	187	314	343	470	515
Y	198	216	370	404	607	665
Z	234	256	474	518	882	966
AA	252	275	497	542	958	1049
BB	325	354	522	569	1170	1282
CC	339	371	524	572	1225	1342
DD	341	373	539	588	1274	1395
EE	371	406	652	710	1658	1814
FF	560	588	749	816	2227	2398
GG	441	484	736	801	2115	2313
HH	488	535	755	821	2297	2511
II	648	710	806	871	2834	3091

REFERENCES

1. Warren, R.S., Gupta, R.R., and Healy, R.D., "Design and Calibration of a Grid Prediction Algorithm for the St. Marys River Loran-C Chain," The Analytic Sciences Corporation, Technical Information Memorandum TIM-1119-2, March 1978. Published as U.S. Coast Guard Report No. CG-D-32-80. Available from the National Technical Information Service, Springfield, Virginia 22161.

2. Johler, J.R., Keller, W.J., and Walters, L.C., "Phase of the Low Radio Frequency Groundwave," National Bureau of Standards Circular 573, June 1956.

3. Shubbuck, T.J., "St. Marys River Loran-C Evaluation," U.S. Coast Guard Research and Development Center, Interim Report No. 2, 30 November 1976.

4. "Final Report on Loran-C Propagation Study," Sperry Systems Management Division, Pub. No. GJ-2232-1892 Rev. A, April 1977.

5. Doherty, R.H., "Spatial and Temporal Electrical Properties Derived from LF Pulse Ground Wave Propagation Measurements," Proc. of the Twentieth Technical Meeting of the Electromagnetic Wave Propagation Panel of AGARD-NATO (Netherlands), March 1974, Paper No. 30.

6. Uttam, B.J. and Gupta, R.R., "Loran-C Additional Secondary Phase Factor (ASF) Correction Algorithm," The Analytic Sciences Corporation, Technical Report TR-735-1-1, October 1976.

7. Bean, B.R. and Dutton, E.J., Radio Meteorology, National Bureau of Standards Monograph 92, Washington, D.C., 1966.

8. Bean, B.R., Horn, J.D., and Ozanich, A.M., Jr., Climatic Charts and Data of the Radio Refractive Index for the United States and the World, National Bureau of Standards Monograph 22, Washington, D.C., 1960.

9. Bean, B.R. and Thayer, G.D., "On Models of the Atmospheric Refractive Index," Proc. IRE, Vol. 47, May 1959, pp. 740-755.

10. "Electrical Characteristics of the Surface of the Earth," Proc. of the Thirteenth Plenary Assembly of the International Radio Consultative Committee (Geneva, Switzerland), 1974, Vol. V, pp. 39-65.

REFERENCES (Continued)

11. Morgan, R.R., "Preparation of a Worldwide VLF Effective Conductivity Map," Westinghouse Electric Corporation, Report No. 80133F-1, March 1968.

12. Fine, H., "An Effective Ground Conductivity Map for Continental United States," Proc. IRE, Vol. 42, September 1954, pp.1405-1408.

13. Hauser, J.P., Garner, W.E., and Rhoads, F.J., "A VLF Effective Ground Conductivity Map of Canada and Greenland with Revisions Derived from Propagation Data," Naval Research Laboratory, Report No. 6893, March 1969.

14. Sage, A.P. and Melsa, J.L., Estimation Theory with Applitions to Communications and Control, McGraw-Hill, New York, 1971.

15. Watt, A.D., Mathews, F.S., and Maxwell, E.L., "Some Electrical Characteristics of the Earth's Crust," Proc. IEEE, Vol. 51, June 1963, pp.897-910.

16. Watt, A.D., VLF Radio Engineering, Pergamon Press, Oxford, England, 1967.

17. Gelb. A. (Editor), Applied Optimal Estimation, MIT Press, Cambridge, 1974.